



UPPSALA
UNIVERSITET

*Digital Comprehensive Summaries of Uppsala Dissertations
from the Faculty of Science and Technology 1568*

Development of Peptide Binders

*Applied to Human CRP, Carbonic Anhydrase (II, IX)
and Lysine Demethylase 1*

JIE YANG



ACTA
UNIVERSITATIS
UPSALIENSIS
UPPSALA
2017

ISSN 1651-6214
ISBN 978-91-513-0086-3
urn:nbn:se:uu:diva-330489

Dissertation presented at Uppsala University to be publicly examined in B/C2:305, Husargatan 3, Uppsala, Thursday, 16 November 2017 at 09:15 for the degree of Doctor of Philosophy. The examination will be conducted in English. Faculty examiner: Professor Morten Grötlí (University of Gothenburg).

Abstract

Yang, J. 2017. Development of Peptide Binders. Applied to Human CRP, Carbonic Anhydrase (II, IX) and Lysine Demethylase 1. *Digital Comprehensive Summaries of Uppsala Dissertations from the Faculty of Science and Technology* 1568. 60 pp. Uppsala: Acta Universitatis Upsaliensis. ISBN 978-91-513-0086-3.

In this thesis, a polypeptide binder concept is illustrated. By conjugation to a set of sixteen polypeptides, a small binding molecule can evolve into a polypeptide binder with increased affinity and selectivity. The concept was applied to 2-oxo-1,2-dihydroquinoline-8-carboxylic acid (DQ) and acetazolamide (AZM) for development of high affinity binders targeting human C-reactive protein (CRP) and human carbonic anhydrase (HCA) II and IX respectively. In addition, peptidic macrocycles were developed as inhibitors of lysine specific demethylase 1 (LSD1).

CRP is a well-known biomarker of inflammation in humans and binders recognizing it are therefore of large interest as medical diagnostics. Until now, phosphocholine (PCh) and derivatives are the only known small molecule binders for CRP, but they have low μM affinity and bind CRP in a Ca^{2+} dependent manner. The small molecule DQ was designed as a CRP binder that is structurally unrelated to PCh. Its polypeptide conjugate, 4-C25I22-DQ, was demonstrated as a strong, Ca^{2+} independent binder for CRP, and had an affinity approximately three orders of magnitude higher than DQ itself.

HCA IX is a protein that is interesting for diagnosis of cancer. AZM is a small molecule inhibitor of HCAs with a dissociation constant of 38 nM for HCA II and 3 nM for HCA IX. Interestingly, polypeptide conjugate 4-C10L17-AZM displayed stronger binding to both HCA II (K_D 4 nM) and HCA IX (K_D 90 pM). This result provided evidence that the binder concept can be applied also for small molecules which already have high affinity for their protein receptors.

LSD1 is an enzyme that regulates the methylation of Lys 4 of histone 3 via a PPI-like interaction and which is of therapeutic interest in certain cancers. Based on the structures of two peptidic ligands bound to LSD1, we sequentially prepared truncated, mono-substituted and macrocyclic peptides in order to develop reversible inhibitors of LSD1. Some stapled cyclic peptides bound to LSD1 with 10-fold higher affinity than the corresponding linear parent peptide. Changing the staple into a lactam further improved the binding potency and the best lactams inhibited the enzymatic activity of LSD1 at low μM K_i values.

Keywords: polypeptide conjugates, molecular recognition, peptide cyclization, protein targets

Jie Yang, Department of Chemistry - BMC, Box 576, Uppsala University, SE-75123 Uppsala, Sweden.

© Jie Yang 2017

ISSN 1651-6214

ISBN 978-91-513-0086-3

urn:nbn:se:uu:diva-330489 (<http://urn.kb.se/resolve?urn=urn:nbn:se:uu:diva-330489>)

*Dedicated to everyone:
Nothing is impossible, the word itself
says 'I'm possible'!*
-Audrey Hepburn

List of Papers

This thesis is based on the following papers, which are referred to in the text by their Roman numerals.

- I Yang, J., Gustavsson, A.-L., Haraldsson, M., Karlsson, G., Norberg, T., Baltzer, L.. High-affinity recognition of human C-reactive protein independent of phosphocholine. *Org. Biomol. Chem.*, **2017**, 15(21): P. 4644–4654.
- II Yang, J., Koruza, K., Fisher, Z., Knecht, W., Baltzer, L.. Improved molecular recognition of Carbonic Anhydrase IX by polypeptide conjugation to acetazolamide, *Bioorganic Med. Chem.*, **2017**, doi: <http://dx.doi.org/10.1016/j.bmc.2017.09.017>.
- III Yang, J., Talibov, V., Geitmann, M., Peintner, S., Poongavanam, V., Rhee, C., Sebastiano, M., Simon, B., Bremberg, U., Henning, J., Danielson, U. H. and Kihlberg, J.. Macrocyclic peptides as inhibitors of human LSD1. Manuscript.

Reprints were made with permission from the respective publishers.

Papers not included in the thesis:

- IV Knecht, W., Eriksson, P.-O., Sandmark, J., Tigerström, A., Blaho, S., Chen, Y., Fex, T., Olsson, T., Rydberg, J., Viljanen, J., Xu, B., Yang, J., Öhman, A., Baltzer, L.. Peptide hybrids of small molecule inhibitor introduce selectivity between kringle domains from Glu-plasminogen and apolipoprotein(a). Manuscript.

Contributions

Paper I and Paper II. Took a part in the molecular design. Performed the whole part of small molecule and peptide synthesis and affinity evaluation. Contributed to the manuscript writing in results and discussions part and corresponding experimental and supporting information.

Paper III. Contribution includes macrocyclic peptide design and synthesis. Co-wrote the manuscript.

Contents

Introduction	13
1.1 Molecular recognition in peptides and proteins	14
1.1.1 Non-covalent bonds	14
1.1.2 Binding in aqueous solution.....	15
1.1.3 Cooperativity.....	15
1.1.4 The polypeptide binder concept.....	16
1.2 Peptide design (Paper I and Paper II)	16
1.2.1 The helix-loop-helix.....	16
1.2.2 The sixteen-membered peptide set.....	17
1.2.3 Enhancing affinity and selectivity by peptide conjugation.....	19
1.3 Cyclic peptides (Paper III)	20
Results and Discussion.....	21
2.1 Polypeptide conjugation of a small molecule from a fragment collection provides a peptide hybrid for diagnostic applications by Ca^{2+} independent targeting of the human C-reactive protein (Paper I)	21
2.1.1 Background	21
2.1.2 Design of a small binder molecule and its conjugate analogue ..	22
2.1.3 Fluorescence based evaluation of affinity.....	27
2.1.4 Characterizing the role of Ca^{2+} in 4-C25L22-DQ - CRP binding	27
2.1.5 Identification of a ligand binding site	28
Summary	28
2.2 The development of an acetazolamide based high-affinity peptide conjugate for Human Carbonic Anhydrase IX recognition (Paper II)	29
2.2.1 Background	29
2.2.2 Small molecule design and synthesis.....	30
2.2.3 SPR screening with immobilized HCA II.....	31
2.2.4 SPR analysis with immobilized peptide conjugates	32
2.2.5 Affinity of AZM for HCA II measured by SPR	34
2.2.6 The affinity of 4-C10L17-AZM to HCA IX and some variants ..	35
Summary	36

2.3 Development of macrocyclic peptide inhibitors of the epigenetic enzyme LSD1 (Paper III)	37
2.3.1 Background	37
2.3.2 Structure based macrocycle design	38
2.3.3 Identification of binding epitopes	40
2.3.4 Macrocycle synthesis	43
2.3.5 Evaluation of macrocyclic peptides	45
Summary	47
Conclusion and Outlook	48
Methods	49
3.1 Peptide synthesis	49
3.2 NMR spectroscopy	50
3.2.1 WaterLOGSY	50
3.2.2 2D Spectroscopy for peptide structural analysis	51
3.3 Fluorescence spectroscopy	52
3.4 Surface Plasmon Resonance	53
Svensk sammanfattning	55
Acknowledgement	57
References	58

Abbreviations

Acm	Acetamidomethyl
Aoc	L-2-amino-octanoic acid
AZM	Acetazolamide
Boc	Tert-butyloxycarbonyl
CD	Circular dichroism
CRP	Human C-reactive protein
Da	Dalton
DCB	1,2-Dichlorobenzene
DCI	N,N'-Diisopropylcarbodiimide
DCM	Dichloromethane
DIPEA	N,N-Diisopropylethylamine
DMSO	Dimethyl sulfoxide
DQ	2-oxo-1,2-dihydroquinoline-8-carboxylic acid
DTT	Dithiothreitol
EA	Ethyl acetate
EDCI	N-(3-Dimethylaminopropyl)-N'-ethylcarbodiimide hydrochloride
EDTA	Ethylenediaminetetraacetic acid
FAD	Flavin adenine dinucleotide
Fmoc	Fluorenylmethyloxycarbonyl
HBS-P	0.01 M HEPES pH 7.4, 0.15 M NaCl, 0.005% v/v Surfactant P20
HCA	Human carbonic anhydrase
HCl	Hydrochloric acid
HCTU	O-(7-azabenzotriazol-1-yl)-N,N,N',N'-tetramethyluronium hexafluorophosphate
HF	Hydrogen fluoride
H3K4	Histone 3 Lysine 4
H ₂ SO ₄	Sulfuric acid
K _D	Equilibrium dissociation constant
LC-MS	Liquid chromatography-mass spectrometry
LSD1	Lysine specific demethylase 1A
LSD2	Lysine specific demethylase 1B
MAO	Monoaminoxidase
MD	Molecular dynamics
MS	Mass spectroscopy

NBS	N-bromosuccinimide
NMR	Nuclear magnetic resonance
NOE	Nuclear Overhauser effect
NOESY	Nuclear Overhauser effect spectroscopy
PBS	Phosphate buffered saline
PC/PCh	Phosphocholine
PDB	Protein data bank
PG	Proteoglycan
PP1	3,5-bis[[bis(2- pyridylmethyl)amino] methyl] benzoic acid
PPIs	Protein-protein interactions
RCM	Ring closing metathesis
RP-HPLC	Reversed phase-high performance liquid chromatography
SPPS	Solid phase peptide synthesis
SPR	Surface plasmon resonance
TFA	Trifluoroacetic acid
TLC	Thin layer chromatography
WaterLOGSY	Water-ligand observed via gradient spectroscopy

20 naturally occurring amino acids:

Amino Acid full name	Three letter	One Letter
Alanine	Ala	A
Arginine	Arg	R
Asparagine	Asn	N
Aspartic Acid	Asp	D
Cysteine	Cys	C
Glutamic Acid	Glu	E
Glutamine	Gln	Q
Glycine	Gly	G
Histidine	His	H

Isoleucine	Iso	I
Leucine	Leu	L
Lysine	Lys	K
Methionine	Met	M
Phenylalanine	Phe	F
Proline	Pro	P
Serine	Ser	S
Threonine	Thr	T
Tryptophan	Trp	W
Tyrosine	Tyr	Y
Valine	Val	V

Introduction

Protein recognition and binding is a most important event in biological processes, including enzymatic catalysis, signal transduction, protein trafficking and immune recognition. In order to better understand the correlation between protein recognition and its associated biological processes, there is an increasing demand for chemists and biologists to develop binders with high affinity and selectivity for proteins of biological interest.

Current binder technologies can be divided into two groups: binders of biological origin or small synthetic molecules. Antibodies remain the golden standard as diagnostic tools in the clinic and are also established as powerful therapeutics. More recently “humanized antibodies”, ankyrin repeats, affibodies derived from protein A and lipochalins that provide additional opportunities have emerged. They are all prepared by protein expression and selected by screening of libraries rather than by design.¹⁻⁴ As the size of the library normally is large, binders having high affinity and selectivity can usually be generated.

Small synthetic molecules that comply with Lipinski’s rule of 5 still constitute the major share of pharmaceuticals.⁵ An important advantage of binders prepared by organic synthesis is that the chemical process eliminates the risk of contamination from other biological sources. The possibility of variation from batch to batch is also reduced. However, much more effort has to be devoted to produce small molecule binders that display affinities and selectivities comparable to antibodies.

The growing interest in understanding the role of protein-protein interactions (PPIs) in the control and modulation of intra- and extra- cellular processes manifests in an increasing need for specific high affinity protein binders in life science. In order to meet this need, chemical space has to be expanded beyond small synthetic molecules and engineered proteins to include other classes of compounds such as macrocycles and peptides.⁶⁻⁸ This thesis describes an affinity enhancer concept explored by our group and its application in the development of high affinity binders for human C-reactive protein (CRP) and human carbonic anhydrase (HCA). In addition, another strategy based on the design of macrocyclic peptide binders for human lysine specific demethylase 1 (LSD1) starting from a native linear peptide is illustrated.

1.1 Molecular recognition in peptides and proteins

Non-covalent interactions are the most important interactions between amino acid residues in peptides and proteins as they provide the stability for secondary structures like helices or sheets. The same aspect is also applied to stabilize the bio-complex formation. In the view of their biological importance, chemists have attempted to both qualitatively and quantitatively investigate the non-covalent interactions in diverse model systems. Their efforts paved the road for us to compile our peptide binder concept, which is to develop high affinity binder by conjugation of polypeptides with small binding organic molecules. Therefore, this section is a brief description of the characteristics of typical almost common non-covalent bonds and their cooperative impact on molecular recognition by using peptides and proteins as models.

1.1.1 Non-covalent bonds

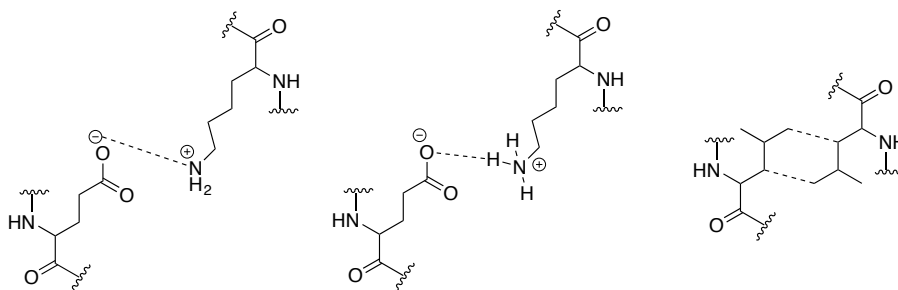


Figure 1. Schematic representation of electrostatic interaction (left), hydrogen bond formation (center) and hydrophobic interactions (right).

In Figure 1 a general description of molecular recognition based on non-covalent bond formation is shown. Compared to covalent bonds (C-H, 416 kJ/mol on average), non-covalent bonds are weak. The bond energy of a salt bridge between a carboxylate ion and an ammonium ion is 20 – 40 kJ/mol. The hydrogen bond varies in strength, with bond energies in the range from 16 to 60 kJ/mol as reflected by the bond distance. The strength of the hydrophobic interactions depends on the surface area involved and provides most of the binding energy in biological systems.

Electrostatic (charge-charge) interaction

At physiological pH in aqueous solution, the side chains of the amino acid residues Lys, Arg and His are typically positively charged whereas the side chains of glutamic acid and aspartic acid are negatively charged. The strength of the interaction is inversely proportional to the distance between the two charged atoms and it is influenced by the nature of environment,

where the interaction is found to be stronger in an apolar environment than in a polar environment.

The hydrogen bond

The hydrogen bond has been the subject of extensive study, and several key reviews are available in the literature.⁹⁻¹² In principle, the hydrogen bond connects two polar atoms ($X = \text{F, O, and N}$) via a hydrogen atom. One polar atom ($X\text{-H}$) acts as the hydrogen bond donor while the other acts as the hydrogen bond acceptor ($\text{H}\cdots\text{X}'$). The donor and the acceptor are not linearly connected via the hydrogen and the bond strength is reflected in the bond length as well as in the bond angle of $X\text{-H}\cdots\text{X}'$.

Hydrophobic interactions

The interface between hydrophobic surfaces is often large and takes place between aliphatic and aromatic substituents. The electronic density fluctuates and transient areas of high or low electron density provide temporary interacting dipoles. The bond strength falls off quickly following a sixth order dependence on interatomic distance and hydrophobic interactions only form at short distances.

1.1.2 Binding in aqueous solution

In aqueous solution, molecules are solvated and the role of water must be included in a discussion on non-covalent interactions. For instance, a salt bridge is weaker in aqueous solution than in a hydrophobic environment. This is because the charge is partially neutralized by the water surrounding it. Similarly, a hydrogen bond is weak because the solute is already hydrogen bonded to water molecules and the net gain in free energy of forming another hydrogen bond is small. The formation of $X\text{-H}\cdots\text{X}'$ can still be energetically favorable, even though there is little change in enthalpy (the number of hydrogen bonds is equal before and after the formation of $X\text{-H}\cdots\text{X}'$) because of the release of bound water molecules. The same principle also applies to hydrophobic interactions where bound water molecules are also released.

1.1.3 Cooperativity

An understanding of the concept of cooperativity is critical for the understanding of the principles behind the polypeptide conjugate binder concept, a core concept in this thesis.

A cooperative system involves a molecule, e.g. protein, with at least two ligand binding sites. It also involves a molecule with two separate functional groups that can bind to both of these sites simultaneously. Binding to one of the ligand binding sites is associated with a free energy of binding, including

an entropy term that is negative due to the loss of the translational degrees of freedom when two molecules form a complex. The binding of the second group to the second ligand binding site does not include to the same extent the negative entropy contribution. It is covalently linked to the first group, and has already lost the degrees of freedom associated with complexation. Weak interactions between the second group and the second ligand binding site can therefore provide significant affinity enhancements, as do those of the polypeptides conjugated to the small organic molecules discussed in this thesis.

Jencks (1981) used an energy model to describe the affinity gain by the cooperativity effect.¹³ For ligands A and B, each one has an “intrinsic binding energy” (ΔG^i_A , ΔG^i_B) that corresponds to the affinity to the receptor. There is a “connection Gibbs energy” (ΔG^S) that is derived largely from changes in translational freedom. By carefully examining several different intramolecular models, the advantage of ΔG^S can be as large as $\approx 10^8$ (M) and has been shown to be $\approx 10^5$ (M).

1.1.4 The polypeptide binder concept

The polypeptide binder molecule is a conjugate formed from a small ligand molecule and a polypeptide selected from a set of sixteen designed sequences connected via an aliphatic spacer. The designed polypeptide itself has some propensity to fold in a helix-loop-helix motif. The structure was not designed to recognize any specific protein, rather the peptide scaffold acts as an affinity enhancer. Principally, it is an entropically driven concept, where the initial binding to the protein by the small molecule ligand makes the subsequent interaction between peptide and protein intramolecular (cf. section 1.1.3). The translational entropic penalty for peptide association has been reduced by conjugation to the small organic ligand, so the additional binding interactions between peptide and protein surface leads to the overall affinity increase. The magnitude of the affinity gain is determined by the strength of the interactions occurring at the peptide-protein interface.

1.2 Peptide design (Paper I and Paper II)

1.2.1 The helix-loop-helix

In the early stage of peptide design, SA-42, a 42-residue polypeptide was designed and synthesized to fold as a helix-loop-helix motif. The structural evidence was obtained from circular dichroism (CD) and NMR spectroscopy. The mean residue ellipticity at 222 nm of SA-42, $-25\,000\text{ deg cm}^2\text{ dmol}^{-1}$ was comparable to that of other published helix-loop-helices.¹⁴ Using SA-42 as a template, KE2 with similar sequence was functionalized with benzene-

sulfonamide, a human carbonic anhydrase II (HCA II) binding molecule with a K_d of 1.5 μ M. Several conjugates were synthesized by varying the length of the spacer. Remarkably, the affinity of the peptide conjugate KE-2 D(15)-8 (K_d = 4 nM) was increased by almost three orders of magnitudes compared to that of the small molecule alone.¹⁵ ¹⁵N NMR spectroscopy revealed that the peptide scaffold also had interactions with the protein. The interface between peptide and protein was located close to the small molecule binding pocket. CD analysis of the KE-2 D(15)-8 – HCA II complex indicated that the helicity of the peptide scaffold was barely effected by binding to the protein. Possibly the helical structure is advantageous in association with the protein surface. Apart from this, the interaction study by SPR revealed that there was no measurable affinity of non-functionalized KE2 D(15)-8 for HCA II. Because the sequence of the parent peptide SA-42 was *de novo* designed, the observed binding phenomenon was ascribed to the cooperativity induced affinity gain. Very likely, the principle behind the high affinity binder for HCA II was hypothesized to be a general aspect to be exploited for other conjugate – protein systems with other ligands tethered to the polypeptide. However, considering the complexity of proteins, one polypeptide scaffold was considered unlikely to be able to bind strongly to any protein. Thus a set of polypeptides was designed with sequences based on that of KE2 in order to develop a binder strategy that would be applicable to a wide range of protein targets.

1.2.2 The sixteen-membered peptide set

The set contains 16 sequences of polypeptides, Table 1. The design of the library has been described previously.^{16,17} Each peptide contains 9-13 Ala residues that are intrinsically prone to form helical structures. The hydrophobic residues, Leu, Ile, Nle and Phe, were eight in total in each sequence. They were placed in a or d positions according to the nomenclature of the heptad repeat in order to form a hydrophobic core to stabilize the helical structure, Figure 2. The remaining positions were filled with polar and charged residues. Gly and Pro that are often found in turn structures were placed in positions 20 and 21 to initiate the formation of a 4-residue turn linking the two helical segments. The sequences were expected to fold as helix-loop-helix motifs in aqueous solution. Structural evidence was provided by CD spectroscopic analysis.^{16,18}

The composition of the library followed two criteria. The first criterion was the ligand conjugation site, where the side chain of a lysine was used to form an amide bond with a modified ligand. The second was the net charge of the peptide sequence. The lysine used for ligand conjugation was situated in position 8, 17, 22 and 34, i.e. in the early and later parts of the N-terminal helix, in the loop region and in the middle of the C-terminal helix. In other words, the sites of incorporation were evenly distributed over the polypep-

tide sequence. The number of Arg and Asp residues was varied as well as the C-terminal charges so that the net charges of peptides were between -7 and +2.

Table 1. The amino acid sequences of the polypeptides in the designed set including the total charges of the binder conjugates.^a

Peptide	Sequence	Global charge
1-C15L8	<i>Ac</i> -NEADLEA K IRHLAE <u>K</u> LEARGPEDCEQLAEQLARAFEAFARKG-OH	-7
1-C10L17	<i>Ac</i> -NAADLEAAIKHLAEAL K ERGPEDCEQLAEQLARAFEAFARKG-OH	-7
1-C25L22	<i>Ac</i> -NEADLEAAIRHLAEALEARGP K DCKQLAEQLARAFEAFERKG-OH	-6
1-C37L34	<i>Ac</i> -NEADLEAAIRHLAERLEARGPADCAQLAEQLAA K FE <u>K</u> FARKG-OH	-5
2-C15L8	<i>Ac</i> -NEADLEA K IRHLAE <u>K</u> LAARGPVDCAQLAEQLARAFEAFARKG-OH	-4
2-C10L17	<i>Ac</i> -NAADLEAAIKHLAEAL K ARGPVDCAQLAEQLARAFEAFARKG-OH	-4
2-C25L22	<i>Ac</i> -NEADLEAAIRHLAEALAARGP K DCKQLAEQLARAFEAFARKG-OH	-4
2-C37L34	<i>Ac</i> -NAADLEAAIRHLAERLAARGPVDCAQLAEQLAA K FE <u>K</u> FARKG-OH	-3
3-C15L8	<i>Ac</i> -NAADJEA K IRHLAE <u>K</u> JAARGPVDCAQJAEQLARRFEAFARKG-NH ₂	-1
3-C10L17	<i>Ac</i> -NAADJEARIKHLAERJ K ARGPVDCAQJAEQLARAFEAFARKG-NH ₂	-1
3-C25L22	<i>Ac</i> -NAADJEAIRHLAERJAARGP K DCKQJAEQLARAFEAFARKG-NH ₂	-1
3-C37L34	<i>Ac</i> -NAADJEAIRHLAERJAARGPVDCAQJAEQLAR K FE <u>K</u> FARKG-NH ₂	-1
4-C15L8	<i>Ac</i> -NAADJEA K IRHLRE <u>K</u> JAARGPRDCAQJAEQLARRFERFARKG-NH ₂	2
4-C10L17	<i>Ac</i> -NAADJEARIKHLRERJ K ARGPRDCAQJAEQLARAFERFARKG-NH ₂	2
4-C25L22	<i>Ac</i> -NAADJEARIRHLRERJAARGP K DCKQJAEQLARAFERFARKG-NH ₂	2
4-C37L34	<i>Ac</i> -NAADJEARIRHLRERJAARGPRDCAQJAEQLAR K FE <u>K</u> FARKG-NH ₂	2

^aThe lysine residue used for coumarin incorporation is shown in *italic*. The fluorophore is incorporated while the polypeptide is still on the solid support and only one lysine is available for ligand conjugation in solution. The lysine used for ligand incorporation is shown in bold face. The lysine at position of 41 is TFA protected. J is norleucine.

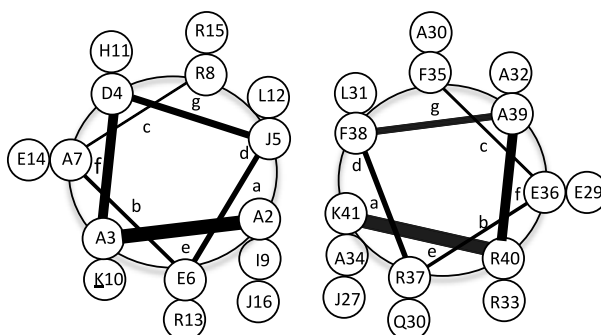


Figure 2. Schematic helical wheel representation of the expected helical segments in sequence 4-C10L17. Residues 2-16 (left) and residues 27-41 (right) are displayed. **K** is the site of incorporation of coumarin, K41 is TFA protected. J is norleucine.

1.2.3 Enhancing affinity and selectivity by peptide conjugation

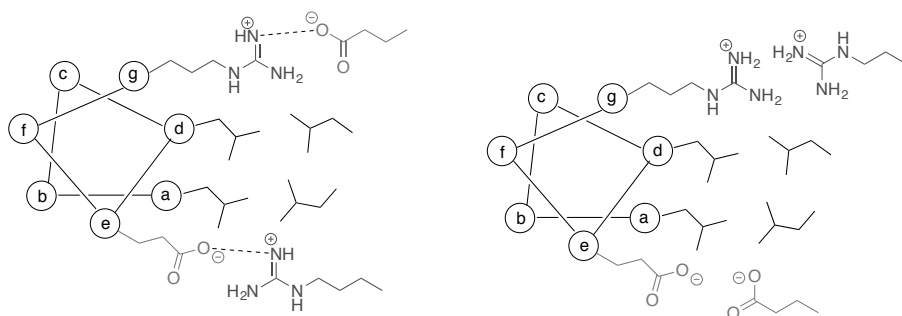


Figure 3. Topological representation of a helical segment interacting with a protein surface. The complementary charge-charge interactions will enhance the binding, whereas unpaired charged residues will repel each other with subsequent effect to the hydrophobic contacts. The largest amount of binding energy is believed to come from hydrophobic interactions.

There is no direct structural evidence to show how the peptide interacts with a protein. Nevertheless the binding is likely to resemble the interactions between proteins. Protein surfaces are not smooth; instead there are many crevices that could form small pockets available for protein-protein interactions.⁸ In contrast to small organic molecule-protein interactions, PPIs typically have larger contact areas in the range of 1 000 – 6 000 Å.^{2,19} However, some residues denoted as hot spots have disproportionally larger energy contributions than other residues. Analysis of alanine scanning data indicates that there is a high preference for Trp, Tyr and Arg in PPIs. Considering the solvation effects on non-covalent interactions in aqueous solution, protein association is probably a process driven by hydrophobic interactions. The polar residues at the interface then provide specificity in the recognition.²⁰ Therefore in the case of polypeptide conjugates the hydrophobic residues are probably responsible for the largest part of the observed affinity increase. Proof for this assumption was obtained from the substitution of hydrophobic residues by Ala which reduced the affinity of the polypeptide conjugate 4-C15L8-PP1 for glycogen phosphorylase a. An attempt to change Leu, Ile into L-2-amino-octanoic acid (Aoc) resulted in an affinity increase by a factor of 10.²¹ There is no direct evidence to show how the peptide conformation is related to the peptide-protein interactions. Possibly the helical structure increases the accessibility of hydrophobic residues in contact with the protein surface. It is likely that the peptide conjugate binding to the protein is initiated by the small ligand binding to its binding site, so that the peptide is brought in contact with the protein surface. The peptide then adapts its structure in order to establish a favorable contact. Presumably hydrophobic side chains first engage in interactions with the protein surface and then the peptide backbone adapts to the local environment of the pro-

tein-peptide binding region. Polar residues form interactions and contribute the binding specificity by charge-charge complementary, Figure 3.

1.3 Cyclic peptides (Paper III)

In addition to development of high affinity binders by conjugating ligands to designed peptides, peptide cyclization based on the crystal structure of protein-peptide complexes was utilized as a means to develop binders in my third paper.

Under physiological conditions native peptides exhibit a wide range of biological properties. In some cases they can be used directly as pharmaceuticals, but often this is not possible. Properties possessed by peptides, such as rapid degradation by proteases, high hepatic clearance, side effects caused by interaction of structurally flexible peptides with other receptors and low membrane permeability are in most cases detrimental to their application as drugs.²²⁻²⁵ Chemical modification of peptides by cyclization often improves bioavailability and metabolic stability and constitutes a simple tactic for the first step in transformation of native peptides into more druglike compounds.

Nowadays, X-crystallography routinely provides high-resolution information about PPIs. This allows facile identification of the peptide sequences that are most important for protein-protein binding, as well as their secondary structures. Cyclization of short synthetic peptides corresponding to such bioactive sequences may force the peptide backbone to fold into bioactive conformations by structural constraints. Different strategies – for example, hydrocarbon bridging by ring closing metathesis (RCM), lactam bridges and triazole linkers – have been reported to afford cyclic peptides that successfully mimic desired backbone structures.²⁵ They all constitute attractive approaches for generation of starting points for peptide based drug discovery projects.

Results and Discussion

2.1 Polypeptide conjugation of a small molecule from a fragment collection provides a peptide hybrid for diagnostic applications by Ca^{2+} independent targeting of the human C-reactive protein (Paper I)

2.1.1 Background

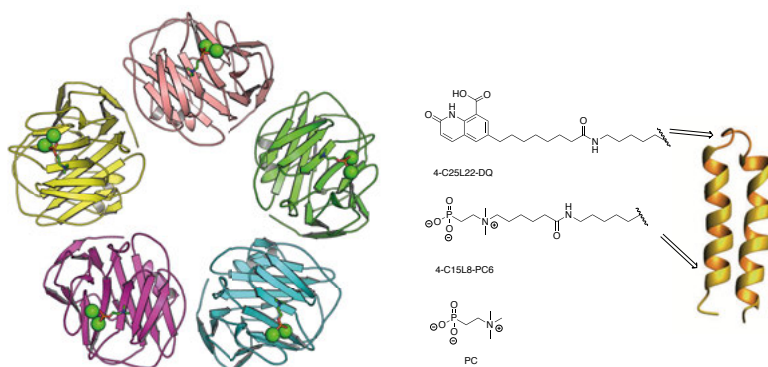


Figure 4. Left: X-ray crystal structure of CRP in complex with Ca^{2+} and PCh, PDB ID: 1B09. CRP backbone is shown as a cartoon model, PCh is shown as a ball-stick model and Ca^{2+} is shown as a sphere model. CRP is composed of five identical subunits connected by non-covalent bonds. Each CRP subunit contains one PCh binding pocket, where two Ca^{2+} are required for PCh binding. Right: Structure of peptide conjugate binder 4-C25L22-DQ with DQ conjugated at the side chain of Lys22, and 4-C15L8-PC6 where PCh is conjugated at the side chain of Lys8.

The human C-reactive protein (CRP) is present in the human serum. Its circulating concentration is an important biomarker to indicate inflammation and the risk of cardiovascular disease.²⁶ In clinical diagnostics, the measurement of the CRP level is typically carried out by using antibodies as the recognition molecule. Nevertheless, there is a need for more chemically stable and easily synthesized organic constructs to meet more challenging requirements, i.e. home testing.

Previously it was demonstrated that a small organic binder molecule, by conjugation to a set of designed synthetic peptides could form hybrid mole-

cules with increased affinity and improved selectivity in comparison to the small molecule alone.^{16,27-30} Among those, 4-C15L8-PC6 formed from a library peptide and the native ligand phosphocholine (PCh, K_D 5 μ M) was reported to bind CRP 1000-fold stronger than PCh alone, demonstrating a binding affinity and selectivity comparable to an antibody towards CRP, Figure 4.¹⁶ The concept has proven to be successful when natural ligands or reported inhibitors were employed. Typically the affinities of the peptide hybrids were increased by 3-5 orders of magnitude over those of the small molecules.^{17,29,30} The attached ligand PCh acts as predominant binding element in the overall interactions between peptide and protein, and therefore calcium is critical for 4-C15L8-PC6 in CRP recognition. EDTA and heparin, which are commonly used to prevent coagulation of blood in diagnostic tests, are not compatible with the use of PCh-dependent agents because they bind Ca^{2+} . The main objective of this project was the development of a new CRP binder playing the same role as 4-C15L8-PC but independent of Ca^{2+} for the binding of CRP. The outcome of an initial literature study showed that there is a lack of small organic molecules that recognize and bind CRP in the absence of Ca^{2+} .^{31,32} A new small organic molecule was required to overcome this problem. By 1H NMR spectroscopy, a set of 18 fragments were screened under Ca^{2+} free conditions and molecules with binding properties were identified and selected for rational design of a new small molecule for CRP recognition. With this molecule, we wanted to demonstrate that novel designed binder molecules as well as known ligands could be attached to the designed peptides and used to form potent recognition elements for proteins.

2.1.2 Design of a small binder molecule and its conjugate analogue

2.1.2.1 Small molecule lead selection by 1H -NMR

From the 18 selected fragments, three were found to interact with CRP using WaterLOGSY 1H NMR, Figure 5. The observation that all three were expelled from CRP by a control molecule indicated that they bound to the same side of the protein and rather close. The three molecules displayed some similar structural elements that were very likely to be essential for their binding to CRP:

1. They all contained a flat bicyclic ring system.
2. Two carbonyl groups flank a heterocycle nitrogen, possibly acting as H-bond acceptors.

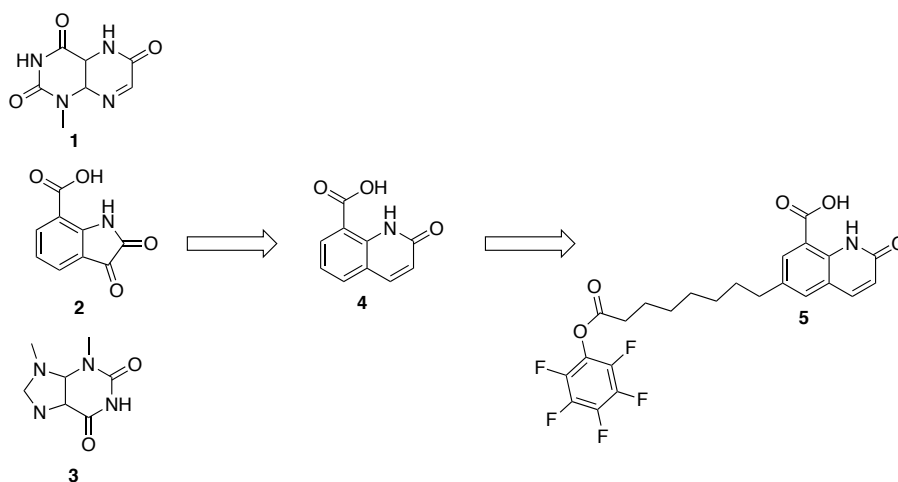
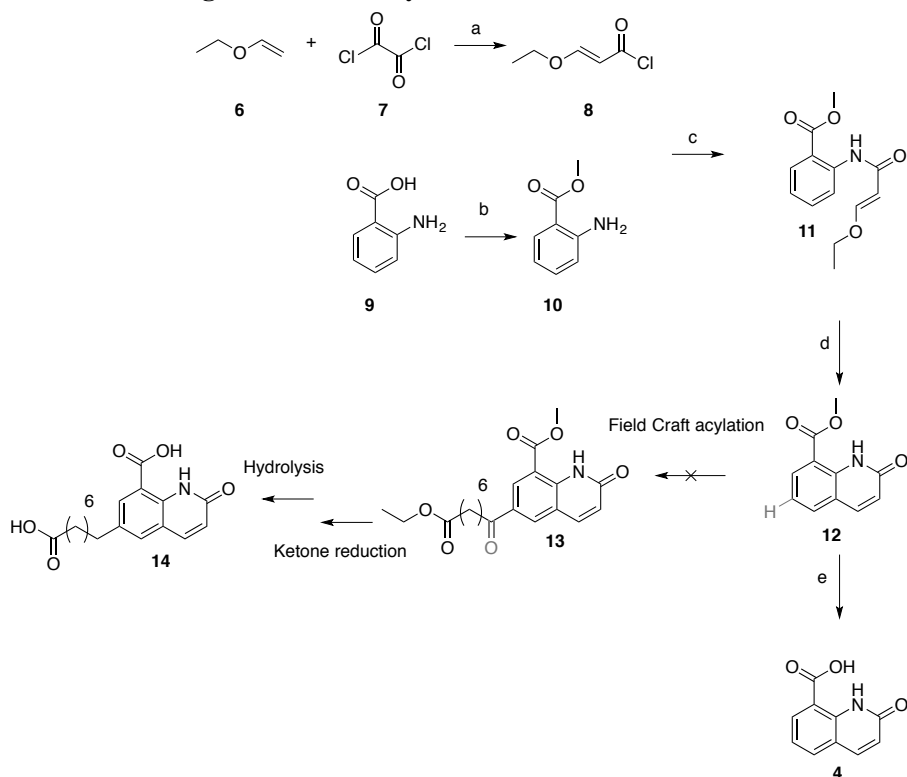


Figure 5. Structures of fragment molecules identified by ^1H NMR spectroscopy (1,2,3), the designed molecule (4) and the modified molecule (5) prepared for peptide conjugation.

Based on these similarities between the three hits the small organic molecule **4** (DQ) was designed and expected to bind to CRP. A spacer was introduced in the position para to the ring NH group to allow conjugation of the organic molecule to the peptides via amide bond formation. The chosen position is in para to the functional groups expected to form binding interactions with the target. The active ester **5** was therefore considered likely to bind in a similar way as **4**. Since the CRP binding site of the three hits were unknown, the length of the spacer was decided based on experience from 4-C15L8-PC. The pockets on the protein surface were shallow, and eight carbon atoms were considered enough to position the small molecule ligand in a binding pocket while the spacer would be flexible enough to allow the polypeptide to dock in the best possible binding site in close proximity to the small molecule binding pocket.

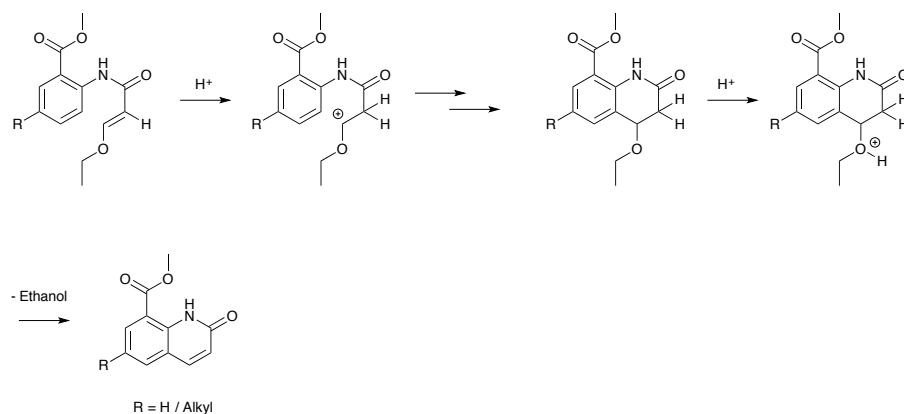
2.1.2.2 Small organic molecule synthesis



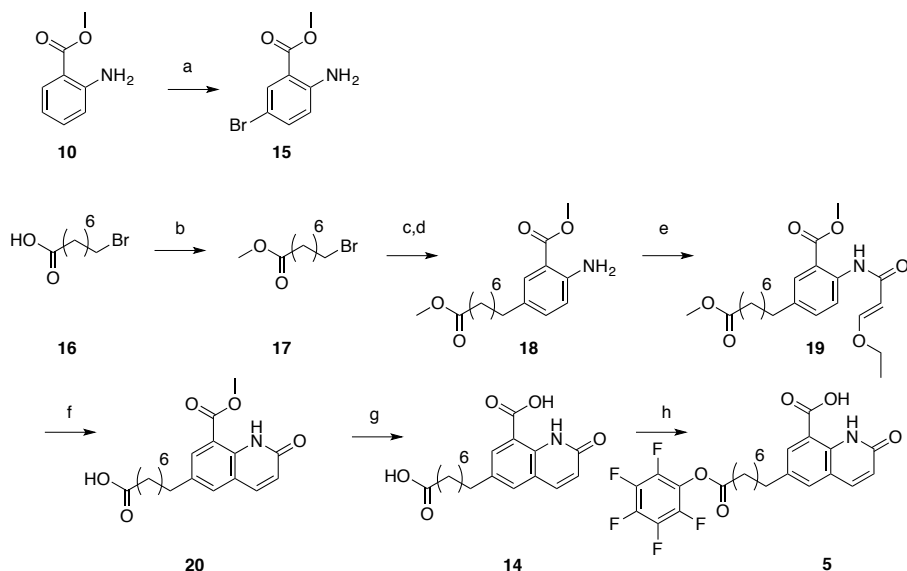
Scheme 1. The first attempts to obtain key derivatives **4** and **14**. *Reagents and conditions:* a, oxalyl chloride, excess; b, thionyl chloride, DCM, then MeOH; c, pyridine, DCM; d, 37 % HCl, r.t. overnight; e, tert-BuOH : H₂O 1:1, reflux 1h.

In a first attempt at preparing the derivatives **4** and **14**, Scheme 1, intermediate **11** was prepared from **6** and **9** in reasonable yield. Acid-catalyzed (95 % H₂SO₄) annulation of **11** gave **12** in only 20 % yield.³³ Interestingly, the yield increased to 38 % when 37 % HCl was used instead of H₂SO₄. Product carbonization with H₂SO₄ could explain the lower yield. Continued hydrolysis afforded **4** in 100 % yield. Attempted Friedel-Crafts acylation of **12** with methyl 8-chloro-8-oxooctanoate to give **13** failed, possibly because of the presence of the deactivating carboxylate group on the aromatic ring. For this reason, it was decided to introduce the spacer by a different synthetic pathway, Scheme 3. The same starting materials **10** and **8** were used, but the hydrogen at the intended spacer attachment site in **10** was replaced with a Br-atom by bromination with N-bromosuccinimide (NBS) to give compound **15**. During this reaction di-bromide side product formation was observed so the reaction time was limited to 2 hours with stoichiometric amounts of NBS. The spacer precursor **17** was prepared from 8-bromooctanoic acid (spacer precursors with other carbon chain lengths could be similarly pre-

pared). In step c, the linker precursor **17** was converted into a zinc complex reagent, which was subsequently reacted with compound **15** in the presence of a palladium (II) catalyst mixture (step d). The product **18** was then N-acylated with **8** to give **19** (step e). In step f, the annulation was first attempted with 37% HCl, but no product formation was observed. However, with 95% H₂SO₄ the desired annulation product **20** was obtained in 12.0 % yield. This indicates that the annulation reaction is not sulphonation promoted. Based on these results, a polar acid mechanism is proposed for the annulation reaction **19** – **20**, Scheme 2. Alkaline hydrolysis of **20** gave the diacid **14**, which was subjected to DCI-promoted esterification with pentafluorophenol (step h). The structure of the product monoester **5** was confirmed by ¹H-NMR spectroscopy, Figure 6. Esterification with the electron-withdrawing pentafluorophenyl group should cause a substantial downfield shift of the adjacent aliphatic methylene proton triplet signals. Therefore, signals A (two lower spectra) are assigned to these protons. An analogous shift is seen going from bromooctanoic acid to its pentafluorophenyl ester (two upper spectra). The proton triplet signals B (two lower spectra), are assigned to the methylene protons that are adjacent to the aromatic ring. The slight downfield shift going from **20** to **5** could be due to **20** being an aromatic methyl ester and **5** being the corresponding acid. From the above considerations it is evident that the pentafluorophenyl ester is situated on the aliphatic chain. Had it been situated on the aromatic ring, none of the methylene triplet signals would have shown such a large downfield shift on pentafluorophenol esterification.



Scheme 2. Proposed polar acidic reaction mechanism for the annulation steps d/f (**11/19** – **12/20**).



Scheme 3. Redesigned synthetic pathway to obtain **5**. Reagents and conditions: **a**, NBS, DCM, reflux 2h; **b**, thionyl chloride, DCM, then MeOH; **c**, Zn, anhydrous LiCl, tertbutyl-silyl chloride, 1,2-dibromoethane, anhydrous THF, 50°C overnight; **d**, **15**, 3 % mol Pd(OAc)₂, 6 % mol S-phos, anhydrous THF; **e**, **8**, pyridine, DCM; **f**, 95% H₂SO₄, r.t. overnight; **g**, tert-BuOH:H₂O 1:1, reflux 1h; **h**, DCI, pentafluorophenol, pyridine, r.t. overnight.

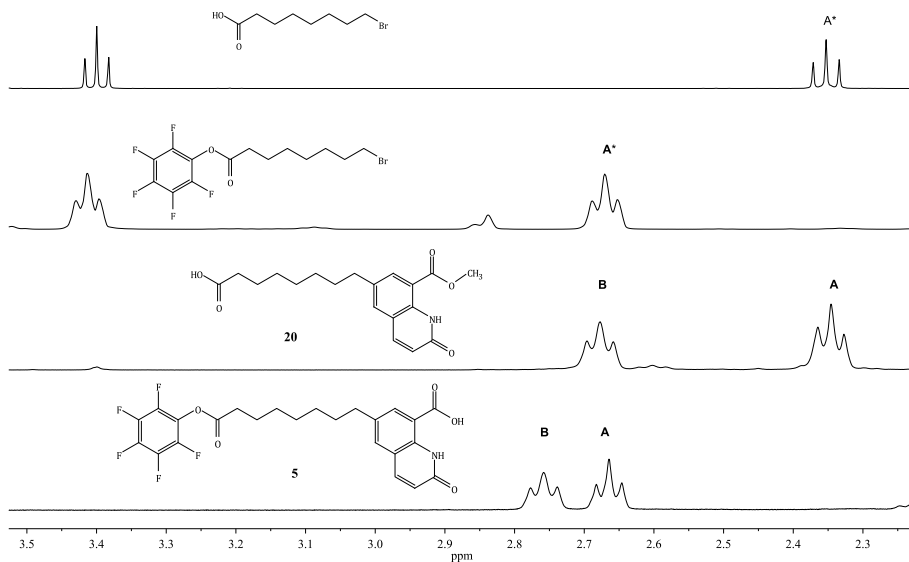


Figure 6. Comparison ¹H NMR spectra of compounds **20** and **5** (two lower spectra). On the carboxylic acid to pentafluorophenyl ester conversion, the carboxyl-adjacent methylene proton triplet, (A) shifted from 2.35 to 2.67. A similar triplet shift on esterification of bromooctanoic acid was seen (two upper spectra). The aromatic-adjacent methylene triplet (B) shifted only slightly from 2.68 to 2.76, probably due to the methyl ester to carboxylic acid change.

2.1.3 Fluorescence based evaluation of affinity

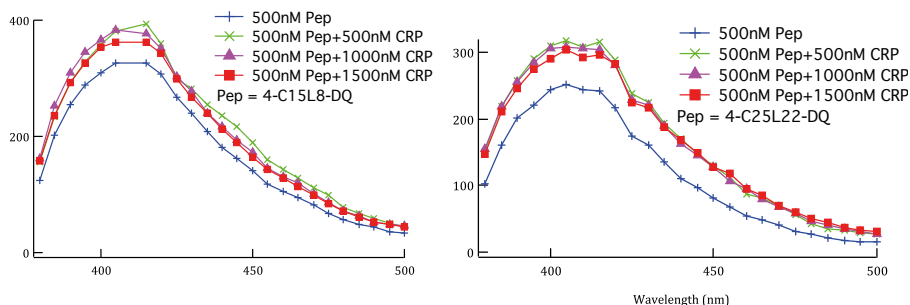


Figure7. Fluorescence emission of peptide conjugates in response to the addition of CRP.

In order to identify the binder molecule with the highest affinity for CRP, a fluorescence titration experiment was carried out with four peptide conjugates each with a global charge of +2. In each peptide, the fluorescent probe 7-methoxycoumarin-3-carboxylic acid was incorporated adjacent to the small molecule ligand. The coumarin probe was expected to be sensitive to the environmental change going from aqueous solution to the protein bound state. The fluorescence emission of the peptide conjugate at 500 nm was found to change in intensity in response to the addition of CRP at concentrations of 500 nM, 1000 nM and 1500 nM. This was taken as evidence of formation of the peptide-protein complex. The intensity change of the emitted light was therefore used to evaluate peptide conjugate affinity for CRP. The results indicated that 4-C25L22-DQ and 4-C15L8-DQ were the tightest binders, Figure 7. Both of them showed a change in intensity upon the addition of 500 nM CRP, but further additions of CRP did not change the emission intensity. In contrast, the other two peptide conjugates did not show saturation of binding at 500 nM concentration of CRP but the emission intensity changed with further additions of protein.

2.1.4 Characterizing the role of Ca^{2+} in 4-C25L22-DQ - CRP binding

CRP binds PCh *in vivo* in the presence of Ca^{2+} under inflammatory conditions. The metal cation concentration increases at the damage site and biological activity of CRP is regulated by the conformational change that occurs upon metal chelation. The reported X-ray crystal structure of the CRP-PCh complex has revealed that two Ca^{2+} ions are accommodated in the vicinity of a shallow hydrophobic pocket in each one of the five identical subunits.³⁴ PCh binds to CRP via a salt bridge between the negatively charged phosphate group and the coordinated Ca^{2+} ions. No other binding sites have been reported for small organic molecules. Consequently, the relationship be-

tween 4-C25L22-DQ and Ca^{2+} with regards to CRP binding was of interest in order to elucidate whether the polypeptide conjugate bound to the PCh binding pocket. If DQ and PCh do not target the same binding site the identification of an unexplored CRP binding site would be of interest to medicinal chemists to unveil where the binding site is and its correlation with a functional role.

The first step was to demonstrate if the binding of 4-C25L22-DQ to CRP required Ca^{2+} ions. An SPR experiment was carried out in the presence and absence of Ca^{2+} , Figure 7 in Paper I. The results revealed that 4-C25L22-DQ is a tight binder for CRP regardless of whether Ca^{2+} is present or not. The dissociation constant was 330 nM in the presence of 10mM CaCl_2 and 760 nM in the absence of CaCl_2 . The small difference may be associated with a conformational change, rather than an effect of Ca^{2+} on binding. Consequently, 4-C25L22-DQ has been shown to bind CRP independent of Ca^{2+} .

2.1.5 Identification of a ligand binding site

As was mentioned above, Ca^{2+} is not important for 4-C25L22-DQ – CRP complex formation but that does not exclude the possibility that DQ binds in the same binding pocket as PCh. Competition for CRP between PCh and 4-C25L22-DQ was therefore evaluated. The results showed that PCh at a concentration of 12.5 mM did not expel 4-C25L22-DQ from CRP, suggesting that DQ and PCh bind at different binding sites.

Summary

CRP is a biomarker for inflammation and cardiovascular disease. A peptide conjugate, 4-C25L22-DQ, was developed as a high-affinity binder for CRP recognition. The small molecule ligand DQ was designed based on the structures of 3 hits from the screening of a set of 18 molecules by ^1H NMR spectroscopy. DQ and the active ester **5** were synthesized and the active ester was conjugated to four polypeptides from a peptide library. The affinities of the four peptide conjugates were evaluated by fluorescence spectroscopy and the results revealed that 4-C15L8-DQ and 4-C25L22-DQ showed the highest affinities. A further affinity measurement was carried out with 4-C25L22-DQ by SPR. In a 1:1 binding model, the dissociation constant of 4-C25L22-DQ bound to CRP was determined to be 330 nM with presence of 10 mM Ca^{2+} , about 2-fold lower than that in the absence of Ca^{2+} showing that 4-C25L22-DQ bound CRP independent of Ca^{2+} . The immobilized 4-C25L22-DQ selectively extracted CRP from human serum, Figure 9 in Paper I, suggesting that 4-C25L22-DQ was a promising recognition tool in diagnostics applications under low Ca^{2+} level conditions. Competition experiments with PCh unveiled that the ligand-binding site was locally separate from that of PCh.

2.2 The development of an acetazolamide based high-affinity peptide conjugate for Human Carbonic Anhydrase IX recognition (Paper II)

2.2.1 Background

In the previous section, CRP was used as a model system to demonstrate that a small organic molecule not previously known to bind the target protein can be used in the design of peptide conjugates for protein recognition. In molecular design, weakly binding molecules are easier to identify than strongly binding ones. Unfortunately they are not always useful and often tagged as failures. An important aspect of the polypeptide conjugate concept is the potential to save failed molecules and develop strong binders based on their structures. In addition, it is also of interest to determine whether the concept is useful also for molecules that already bind strongly. If it is, how much can the affinity of a strong binder be increased by polypeptide conjugation. With this aim, an AZM derived peptide conjugate was developed for the recognition of HCA II and HCA IX.

Carbonic Anhydrase is an ubiquitous enzyme that catalyzes the reversible hydration reaction of carbon dioxide. There are 15 isozymes present in humans distributed in different organs. Some HCAs have been demonstrated to be involved in disease, and their inhibition is of interest in drug development. HCA IX is a membrane-bound enzyme overexpressed in hypoxic tumors and HCA IX inhibitors have been demonstrated to suppress tumor growth.^{35,36} HCA IX has been suggested to be a useful biomarker in oncology. Among the inhibitors of HCA IX, AZM is of interest due to its high affinity, $K_i = 25$ nM.³⁷ However, clinical applications are limited by its poor selectivity. AZM shows similar affinities for HCA I, HCA II and HCA IX, suggesting severe off-target effects. AZM was therefore considered a good candidate for polypeptide conjugate design. Peptides do not penetrate cell membranes well, and an AZM-peptide conjugate was suggested to target the extracellular HCA IX, while not binding to HCA I and HCA II that reside inside the red blood cells. If successful, the incorporation of reporter groups would allow a number of bioanalytical applications, *in vitro* as well as *in vivo*. The reported dissociation and inhibition constants of AZM to HCA II and HCA IX are in the low nM range, and conjugation to the peptides was expected to increase affinities to the pM level. As a consequence, the dansyl and coumarin-fluorophores were not suitable for affinity determination by fluorescence titration. The conjugates were instead evaluated by surface plasmon resonance (SPR), as it is a more sensitive tool for high affinity measurements. HCA IX is difficult to express, whereas HCA II, which resembles the catalytic domain of HCA IX, is commercially available. For this reason, HCA II was used to evaluate the affinities of peptide conjugates. While there is no reason to assume that the polypeptide conjugate with the

highest affinity for HCA II would also bind the most strongly to HCA IX it was also analyzed by SPR in a preliminary evaluation.

2.2.2 Small molecule design and synthesis

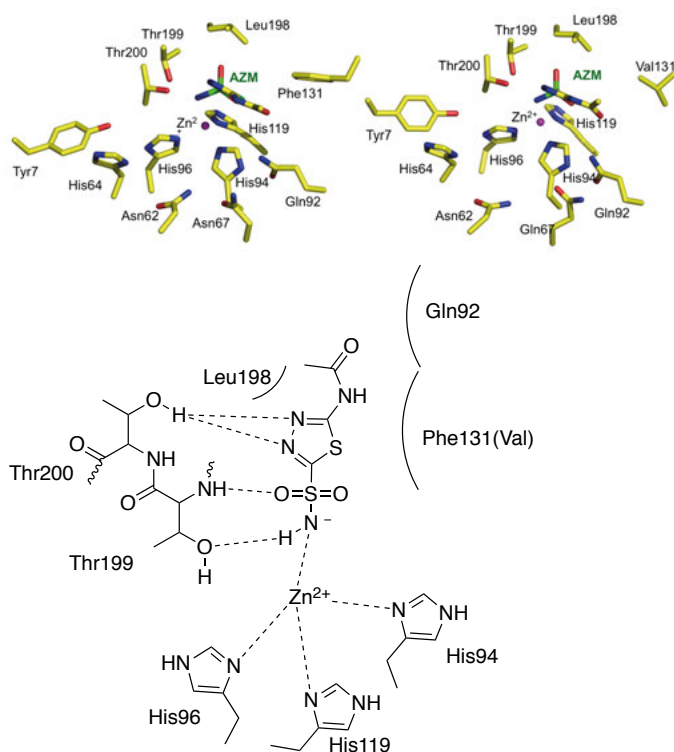
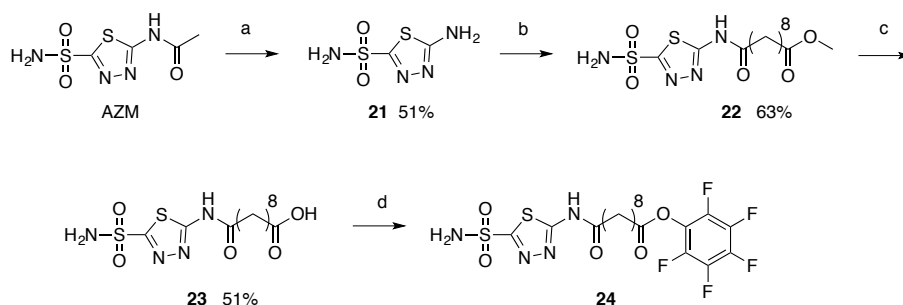


Figure 8. Top left: Detail from the crystal structure of the HCA II AZM complex, PDB ID 4G0C. Top right: Detail from the crystal structure of the HCA IX-AZM complex, PDB ID 3IAI. Bottom: Schematic representation of the binding interactions of AZM in the HCA II and HCA IX active sites.

In order to conjugate AZM to a lysine side chain of the peptide scaffold, an aliphatic spacer was incorporated to allow covalent bond formation. The crystal structures of HCA II and HCA IX complexed to AZM, Figure 8, illustrate that the predominant binding interactions are those between the sulfonamide nitrogen and the active site Zn²⁺ ion, coordinated to the enzyme residues His94, His96 and His119. Additional binding interactions are due to hydrogen bonds with Thr199 and Thr200, hydrophobic and polar contacts between the thiadiazole ring and the side chains of Phe131 (Val) and Gln92. Because the Zn²⁺ ions are located in deep pockets, the sulfonamide group requires a spacer to connect it to the polypeptide that binds to the protein surface. The acetyl group is directed towards the opening of the pocket, and the amide group is thus a suitable position for spacer introduction. The crys-

tal structure shows that the zinc ion is located in a 15Å depth pocket, and a dicarboxylic acid spacer with eight methylene groups was estimated to be large enough to accommodate polypeptide interactions as well as sulfonamide coordination to the active site Zn^{2+} ion.

The structure and synthesis of a designed AZM analogue **24**, with a spacer arm for peptide conjugation, is shown in Scheme 4. In step a, hydrolysis of AZM is performed in 6M HCl to form the primary amine **21**. In step b, an aliphatic 10-carbon spacer is attached to **21** via acylation of the ring nitrogen with methyl 10-chloro-10-oxodecanoate to form the methyl ester **22**. No acylation of the sulfonamide nitrogen was observed either by TLC or LCMS. After hydrolysis of the methyl ester **22** (step c) the acid **23** is converted to the active ester **24** by reaction with pentafluorophenol and EDCI in pyridine (step d). Because of the presence of the sulfonamide group, each intermediate in the synthesis could be isolated as the hydrochloride salt and then recrystallized. The final product **24** was obtained after workup in pure form (by LCMS or ^{13}C NMR) without the need for chromatography.



Scheme 4. Structure and synthesis of **24**. *Reagents and Conditions:* a. 6 M HCl, reflux, 2 hours; b. methyl 10-chloro-10-oxodecanoate, pyridine, acetonitrile, 2 hours; c. 5 % NaOH, 30 minutes; d. pentafluorophenol, EDCI, pyridine, overnight.

2.2.3 SPR screening with immobilized HCA II

An evaluation of the affinities of peptide conjugates with global charges of +2 for HCA II were carried out by SPR, Table 2 and Table 1 (entry 13-16). These polypeptides were selected because in a previous study of benzenesulfonamide derived peptide conjugates, sequences with global charges of +2 showed the strongest binding possibly because the local surface charge was negative, Figure 9.²⁸ Among these four conjugates, 4-C10L17-AZM was estimated to be the strongest binder from the low dissociation rate constant. Based on the crucial K_D values provided from screening, a new SPR experiment was carried out to determine the dissociation constant of 4-C10L17-AZM for HCA II. The result revealed that the K_D was 4 nM, Figure 4 in Paper II.

Table 2. Thermodynamic data of peptide conjugates with global charge of +2 with immobilized HCA II.^a

Peptide conjugate	$k_a/M^{-1}s^{-1}$	$SE(k_a)$	k_d/s^{-1}	$SE(k_d)$	K_D
4-C15L8-AZM	1.56E+05	1.93E+03	2.52E-03	4.03E-05	1.62E-08
4-C10L17-AZM	2.64E+05	3.83E+03	1.90E-03	8.99E-05	7.20E-09
4-C25L22-AZM	9.13E+04	1.78E+03	2.44E-03	1.20E-04	2.67E-08
4-C37L34-AZM	1.20E+05	1.51E+03	2.25E-03	3.13E-05	1.88E-08

^aThe data were obtained by fitting a kinetic equation to the SPR sensorgrams. Each polypeptide conjugate was assayed at concentrations of 0.24 nM, 0.97 nM, 3.9 nM, 15.6 nM and 62.5 nM.

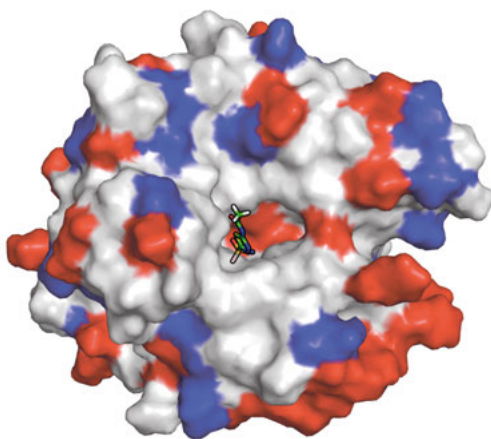
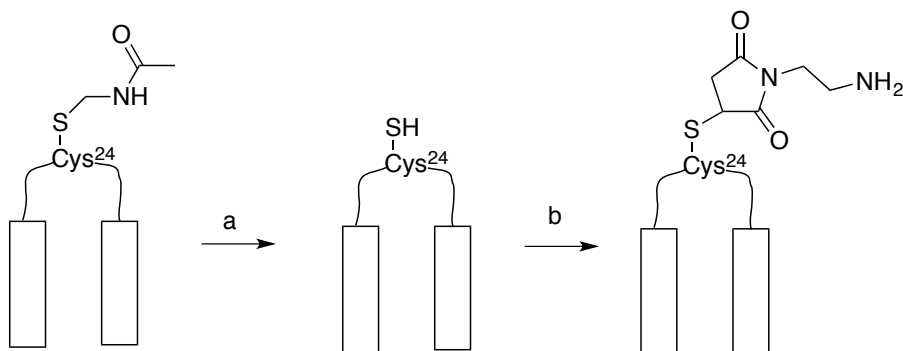


Figure 9. Crystal structure of HCA II in complex with AZM. The positively charged residues are shown in red. The negatively charged residues are shown in blue. The surface close to the binding pocket presents more negative charge, suggesting that the protein-peptide binding is preferred to the positively charged polypeptide conjugates.

2.2.4 SPR analysis with immobilized peptide conjugates

In SPR experiments, normally the protein is immobilized on the sensor chip and the ligand is injected over a range of concentrations. But HCA II is a pH sensitive enzyme and harsh regeneration methods are required to remove the ligands in the case of tight binders. A mild but tedious way to regenerate the chip is by buffer flush. The screening of all peptide conjugates takes a long time and there is a risk that the enzyme will deteriorate with time. The screening of the peptide conjugates was therefore carried out in an inverse set-up, with the peptide conjugate immobilized on chip. The results from the inverse model should not deviate from those with the protein immobilized. Since the peptide conjugates are more robust, harsh regeneration conditions can be used.

2.2.4.1 Modifying peptide conjugate for immobilization



Scheme 5. Reactions used in the functionalization of the polypeptide conjugate.
Reagents and Conditions: a. silver triflate, cold TFA; DTT, 35 % aqueous acetic acid; b. 1-(2-Aminoethyl)-pyrrole-2,5-dione hydrochloride, DMSO.

The polypeptide is readily functionalized and the amino acids Cys²⁴ and Lys⁴¹ are orthogonally protected for this purpose. Modifying Cys²⁴ or Lys⁴¹ of the peptide conjugate is less likely to impact the binding interactions. In order to immobilize the peptide conjugate on the SPR sensor chip, the acetamidomethyl group (Acm) on the side chain of Cys²⁴ was selectively removed by treatment with silver triflate in cold TFA, followed by DTT/aq. acetic acid and purification by RP-HPLC. In the subsequent step the free thiol group was reacted with the maleimide group of the bifunctional linker 1-(2-aminoethyl)-pyrrole-2,5-dione hydrochloride, to provide a primary amine capable of reaction with the free carboxylic acids of the sensor chip hydrogel by standard amide coupling. The overall yield of polypeptide-linker conjugate after purification was approximately 50%.

2.2.4.2 SPR screening

In order to rank the polypeptide conjugates, HCA II was injected in the running buffer at concentrations of 1, 10 and 100 nM, Table 3. The validity of data in the inverse model was confirmed by comparing K_D of 4-C10L17-AZM and 4-C37L34-AZM with those obtained in the protein immobilized binding model. The similarity between the dissociation constants of these two sequences showed that immobilization of the peptide conjugates did not give rise to altered affinities. The results indicated that 4-C10L17-AZM and 3-C37L34-AZM were the strongest binders, but with no more than an order of magnitude affinity difference compared to AZM alone. Comparing these two, the slower off-rate of 4-C10L17-AZM made it the conjugate of choice for further investigations.

Table 3. Thermodynamic parameters of immobilized peptide conjugates with global charges of -4, -1 and +2 with HCA II in the running buffer.^a

Peptide conjugate	$k_a/M^{-1}s^{-1}$	k_d/s^{-1}	K_D/M
2-C15L8-AZM	1.03E+05	3.57E-03	3.46E-08
2-C10L17-AZM	1.19E+05	3.61E-03	3.03E-08
2-C25L22-AZM	5.66E+04	4.37E-03	7.72E-08
2-C37L34-AZM	1.37E+05	3.44E-03	2.52E-08
3-C15L8-AZM	1.57E+05	3.43E-03	2.18E-08
3-C10L17-AZM	1.11E+05	4.09E-03	3.70E-08
3-C25L22-AZM	8.11E+04	4.73E-03	5.83E-08
3-C37L34-AZM	1.84E+05	1.07E-03	5.84E-09
4-C10L17-AZM	1.33E+05	7.62E-04	5.75E-09
4-C37L34-AZM	1.08E+05	1.94E-03	1.79E-08

^aThe data were obtained by fitting a kinetic equation to the SPR sensorgrams. Each sequence was assayed at concentrations of protein of 1 nM, 10 nM and 100 nM.

2.2.5 Affinity of AZM for HCA II measured by SPR

The affinity of AZM for HCA II was determined in an SPR experiment, carried out by flowing a pre-incubated AZM-HCA II solution over 4-C10L17-AZM immobilized on the chip. Because AZM and HCA II are constantly injected in the running buffer the response signal reveals the concentration of the free HCA II that is in equilibrium with AZM. Therefore in this analysis the AZM-HCA II binding affinity can be obtained from the following equation.

$$K_D = IC_{50} - \frac{1}{2}C \quad \text{Eq.1}$$

Here IC_{50} is the total concentration of AZA, at which half of the HCA II is complexed to AZA and C is the total concentration of HCAII. At IC_{50} $C/2$ is equal to the amount of AZA that is bound to HCA II. $IC_{50} - C/2$ is therefore the concentration of free AZA. $K_D = [HCA II]_{\text{free}} * [AZA]_{\text{free}} / [AZA \cdot HCA II]$, and when $[HCA II]_{\text{free}}/[AZA \cdot HCA II]$ equals 1, $K_D = [AZA]_{\text{free}}$ which is $IC_{50} - C/2$.

A sigmoid-shaped inhibition curve indicated that AZM competitively inhibited the 4-C10L17-AZM-HCA II complex formation at μM concentrations, Figure 10. From these measurements AZM was estimated to bind to HCA II with an affinity of 37.5 nM. Since 4-C10L17-AZM was determined to bind to HCA II with an affinity of 4nM, a 10-fold increase in affinity was obtained by polypeptide conjugation. The results illustrate that the small molecule interactions are responsible for most of the affinity, while the affinity enhancement is due to favorable interactions between the protein and peptide components.

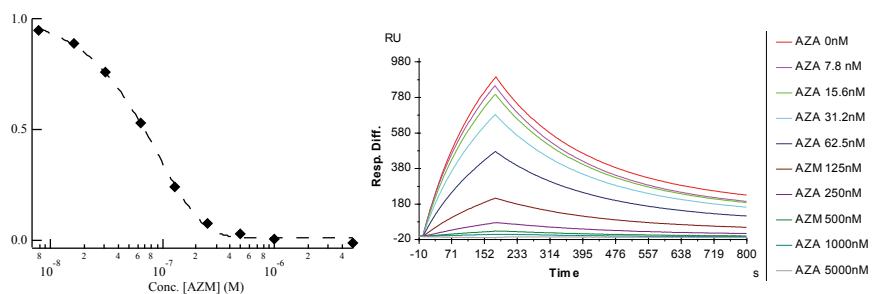


Figure 10. Left: Normalized level of 4-C10L17-AZM – HCA II complex formation as a function of the concentration of AZM pre-mixed with HCA II. [HCA II] was kept fixed at 50nM. Right: Sensorgrams showing AZM-HCA II interactions with 4-C10L17-AZM immobilized.

2.2.6 The affinity of 4-C10L17-AZM to HCA IX and some variants

HCA IX is a membrane bound protein that is overexpressed in some tumor cells, suggesting that HCA IX can serve as a biomarker in oncology. Most molecules developed for HCA IX recognition are based on the structure of HCA II. This is because the sequences of the catalytic domains are highly homologous in HCA IX and HCA II.

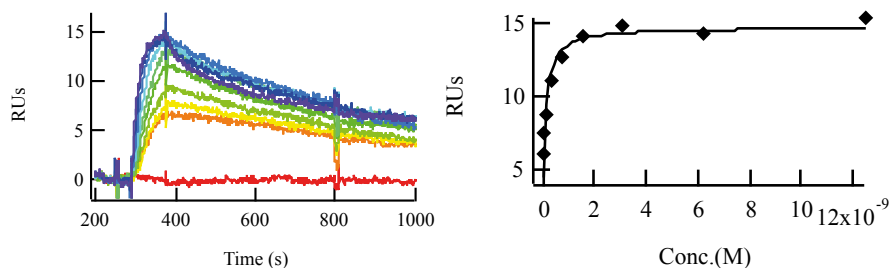


Figure 11. SPR sensorgrams showing interactions between immobilized HCA IX and 4-C10L17-AZM at concentrations of 48.7 pM, 97.5 pM, 195 pM, 390 pM, 780 pM, 1.56 nM, 3.12 nM, 6.25 nM and 12.5nM in HBS-P buffer with 3% DMSO, at pH 7.4. The best fit of an equation describing a 1:1 equilibrium to the maximum responses as a function of the concentration of 4-C10L17-AZM gave a K_D of 90 pM.

While there is no reason to assume that a polypeptide conjugate that binds strongly to HCA II should also bind equally strongly to HCA IX 4-C10L17-AZM, the conjugate with the highest affinity for HCA II was also evaluated with regards to affinity for HCA IX. An SPR experiment was performed using immobilized HCAIX and the same protocol as with HCA II. Assuming a 1:1 binding model, 4-C10L17-AZM was found to bind to HCA IX with a K_D of 90 pM, Figure 11. The affinity was increased by a factor of 33 in comparison to AZM. An investigation of the interactions between 4-

C10L17-AZM and HCA IX variants, Table 4, suggested strongly that the binding enhancement was due to the favorable interaction between the peptide component and residues in the HCA IX proteoglycan domain (PG).

Table 4. Thermodynamic parameters determined for interactions between 4-C10L17-AZM and HCA IX, HCA IX SV, HCA IX mimic and HCA II.^a

	4-C10L17-AZM	AZM
HCA IX	0.09 ± 0.014 nM	3 ± 0.6 nM
HCA IX SV	1 ± 0.7 nM	3 ± 1.0 nM
HCA IX mimic	1 ± 0.3 nM	0.6 ± 0.3 nM
HCA II	4 ± 1.1 nM	38 nM

^aHCA IX contains the active site and proteoglycan (PG) domains present on the extracellular side but not the transmembrane helix and intracellular domains. HCA IX SV is the extracellular domain of HCA IX without the PG domain but with six surface mutations to aid crystallization. HCA IX mimic is a mutant of HCA II with its active site identical to that of HCA IX.

Summary

An acetazolamide analogue, **24**, with a 10 carbon atom spacer was designed and synthesized. It was conjugated to designed peptides with global charges from -5 to +2. All conjugates displayed similar association rate constants while 4-C10L17-AZM showed an order of magnitude slower off-rate than the other candidates. 4-C10L17-AZM binds to HCA II with a dissociation constant of 4 nM and the peptide conjugation increased the affinity by a factor of ten. Moreover, AZM completely inhibits peptide-protein complex formation at μ M concentrations. With respect to HCA IX, 4-C10L17-AZM is also a strong binder, with a dissociation constant of 90 pM, a 33-fold increase over that of the AZM alone. In contrast, no or small binding enhancement was observed for the HCA IX variants that lack the PG-domain of HCA IX. The results suggested that the affinity enhancement was due to interactions between the PG-domain and polypeptide component of the conjugate. Because HCA IX is a membrane bound protein overexpressed in hypoxic tumor cells, 4-C10L17-AZM is of interest in the detection of the HCA IX biomarker. Currently developed small organic molecules do not discriminate between HCA IX and HCA I and HCA II. 4-C10L17-AZM displayed 90 pM affinity and as it is not expected to penetrate cell membranes, better selectively than observed for small organic molecules would be assumed. The use of 4-C10L17-AZM as a recognition element for tumor imaging or other HCA IX targeting applications is therefore promising.

2.3 Development of macrocyclic peptide inhibitors of the epigenetic enzyme LSD1 (Paper III)

2.3.1 Background

Lysine demethylase 1 (LSD1) is an epigenetic enzyme that catalyzes the demethylation of methylated lysine 4 in histone 3 (H3K4), which is a known transcription-activating chromatin mark at gene promoters. In line with this, several studies have found that LSD1 is overexpressed in ovarian, hepatocellular, lung and breast cancers.³⁹⁻⁴² Consequently, inhibitors targeting LSD1 have potential for development into drugs for treatment of cancer.

Monoaminoxidase (MAO) inhibitors were the first class of LSD1 inhibitors to be discovered, which is not unexpected as MAO is structurally related to LSD1. Tranylcypromine, phenelzine and pargyline are members of this class, which are mechanism-based inhibitors.⁴³⁻⁴⁵ Other irreversible inhibitors have also been reported, but appear not to have been optimized for selectivity over LSD2. Thus, they may carry risks of idiosyncratic toxicity resulting from covalent linkage to other proteins.⁴⁶ The discovery of reversible and selective inhibitors has therefore been initiated. Among them, polyamine derivatives, as well as pyrimidine- and triazole-scaffolds have shown modest (μM) potencies and MAO selectivities.⁴⁷⁻⁵⁰ Recently, a series of inhibitors based on indene-containing benzohydrazides having strong (nM) inhibitory potencies for LSD1, and high selectivities against MAO A and B were reported.⁵¹ Thus, they constitute a promising starting point for development of drugs targeting LSD1.

A linear peptide (pM4) containing the 21 N-terminal residues from histone 3, but with Lys4 replaced by Met4, has been reported to be a potent inhibitor of LSD1 with a K_i of 50 nM.⁵² The structure of pM4 bound to LSD1 has been published, just as several structures of related peptides, making pM4 a suitable starting point for development of less peptidic and more drug-like inhibitors of LSD1. We therefore decided to take a structure-based approach, aiming to reduce the molecular weight of the inhibitors, and to improve their potency by conformational restriction. If successful the resulting macrocyclic peptides would constitute a first step towards development of peptidomimetic inhibitors of LSD1.

2.3.2 Structure based macrocycle design

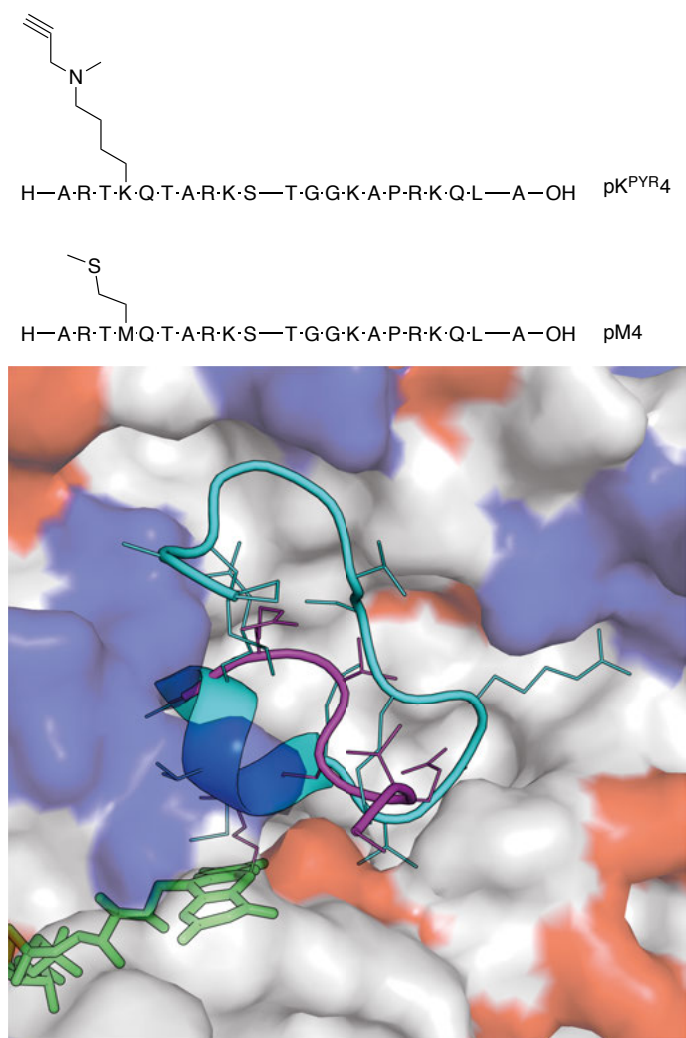


Figure 12. Top: Sequences of peptides pM4 and pK^{PYR}4, which are derived from the N-terminus of histone 3. Bottom: Overlay of the crystal structures of pM4 (in cyanide, PDB ID: 2V1D) and pK^{PYR}4 (in magenta, PDB ID: 2UXN) in complex with LSD1.^{52,53} LSD1 is shown as a surface model, where positively charged residues have been colored in red and negatively charged ones in blue. The FAD cofactor of LSD1 is buried in the depth of the catalytic binding pocket and has been colored in green.

We based our design of cyclic peptides on the structures of the complexes between LSD1 and pM4 and between LSD1 and pK^{PYR}4 respectively, Figure 12. The main reason for choosing these two peptide-LSD1 complexes is because they are both derived from the same parental histone 3 peptide sequence, but display diverse secondary structures. The structural diversity is

caused by the residue at position 4 of the two peptides. For pM4, Met4 is involved in a non-covalent contact with LSD1, whereas a covalent bond is found between the side chain of K^{PYR}4 and the FAD moiety. It is not unexpected that LSD1 can accommodate peptides in different bound conformations, as its catalytic pocket is relatively large and deep, with a funnel-like shape. In addition, this allows LSD1 to perform demethylation on different protein substrates.⁵⁴ It is difficult to conclude whether the pM4 or pK^{PYR}4 complex represents the real conformation of histone 3 when bound to LSD1. We therefore decided to base our design on both structures and to implement different cyclization strategies for them.

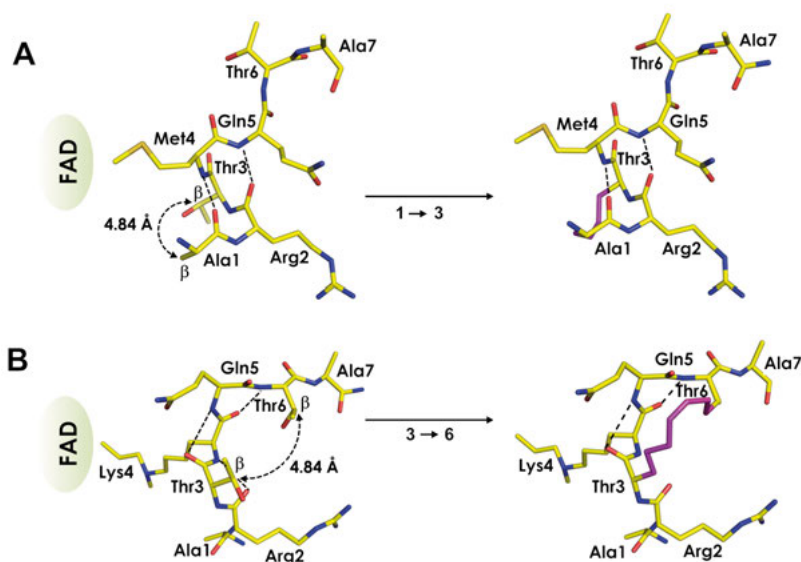


Figure 13. Design of macrocyclized peptides mimicking the secondary structures of linear peptides H3 pM4 and H3 pK4^{PYR} when bound to LSD1. **A)** Structure of H3 pM4 showing the close spatial proximity of the side-chains of Ala1 and Thr3 (left) and how these residues may be linked by a 4-carbon atom bridge (right). **B)** Structure of H3 pK4^{PYR} showing the close spatial proximity of the side-chains of Thr3 and Thr6 (left) and how these residues may be linked by an 8-carbon atom bridge (right). Distances between the β -carbons of the residues to be connected by bridges are given for both structures. Backbone intramolecular hydrogen bonding is indicated by dashed lines. The bridged structures have been energy minimized by MD simulations (Molecular Operating Environment (MOE), 2013.08, CCG, ULC, Montreal, QC, Canada).

For the pM4 complex, the N-terminus of the peptide has folded into a helical turn structure that allows the positively charged N-terminal amino group and the side chain of Arg2 to bind in an anionic pocket in LSD1. The side chain of Met4 is directed towards to the FAD, contributing hydrophobic interactions in another pocket. Beyond the 7 N-terminal residues the rest of the

residues in pM4 are less involved in binding to LSD1. Consequently, cyclization should be performed in the N-terminal region that is located deeper in the binding site of LSD1. As the side chains of Ala1 and Thr3 are sterically close, tethering of them via side chain to side chain cyclization could reinforce formation of a helical turn at the N-terminus, thereby improving the affinity for LSD1.

For pK^{PYR}4 only the first 7 amino acid residues could be detected in the complex with LSD1. Within this segment, the peptide backbone displays three consecutive γ turns, which position the N-terminus and Arg2 in the anionic pocket in approximately the same manner as for pM4. Just as for pM4 the side chain of pK^{PYR}4 is directed towards the FAD moiety, in this case via a covalent bond. In addition, the methylene groups of pK^{PYR}4 form hydrophobic contacts in the pocket containing FAD. Interestingly, the side chains of Thr3 and Thr6 form a polar contact via a bound molecule of water, implying that Thr3-Thr6 cyclization is a viable strategy for conformational restriction.

Molecular dynamics simulations were performed for peptides cyclized by alkyl chains to probe the length of bridge required for conformational restriction, Figure 13. The analysis implied that 4-6 atoms were required to connect Ala1 and Thr3, whereas 6-8 atoms were required for Thr3-Thr6. It is also of interest to investigate whether the bridge is involved in intra- and/or intermolecular interactions (cf. section 2.3.5). To this end cyclic peptides having alkene, lactam and 1,2,3-triazole bridges were prepared and evaluated.

2.3.3 Identification of binding epitopes

Table 5. Affinity data for binding of the pM4 peptide (**1**), and truncated versions, to LSD1 determined by SPR.

Code	Sequence	Length	K _D (μM)
1	H-ARTMQ TARKS TGGKA PRKQL A-OH	21	0.14
2	H-ARTMQ TARKS TGGKA-OH	15	5
3	H-ARTMQ TARKS TGG-OH	13	36
4	H-ARTMQ TARKS T-OH	11	140
5	H-ARTMQ TARK-OH	9	>500
6	H-ARTMQ TA-OH	7	>800

When embarking on design of drug molecules, it is important to establish which are the structural elements that are most important for binding to the target early in the project. For design of small organic molecules that comply with Lipinski's rule of 5, the main focus is on the intermolecular interactions with the target.⁵⁵ However, larger and more complex ligands such as pep-

tides potentially have greater conformational flexibility. For them, defining intramolecular interactions that are important for their secondary structure should be also considered in an essential step of binding epitope identification.

As discussed above the first five-seven residues in the N-terminal region of peptide pM4 (**1**, Table 5) display an ordered helical secondary structure and contacts LSD1 in the crystal. By contrast, the residues towards the C-terminus make fewer contacts with the surface of LSD1, but are instead involved in intramolecular interactions with the N-terminus of **1**, for instance Arg2-Gly12 and -Gly13, Gln5-Ser10, Figure 14. The tail part, i.e. residues 12–16 are also more exposed to solvent in the crystalline complex with LSD1. Consequently, the C-terminal tail has been hypothesized to be less important for binding to LSD1.^{52,56} However, as this hypothesis has not been experimentally verified we prepared a series of peptides that were truncated from the C-terminus, Table 5.

Truncation to give peptides **2** and **3** resulted in a 35 to 250-fold loss in binding affinity for LSD1, as determined by SPR. Moreover, peptide **6** which only contains the N-terminal residues that make the majority of contacts with LSD1 has lost affinity by >5700 fold, and displays almost no binding. These observations illustrate the important role that intramolecular interactions may have in binding of peptides to their targets and highlight the need to consider them in compound design, Figure 13. We propose that such interactions may compensate for the entropic cost required to order the peptide into the secondary structure required for the N-terminal segment to bind in the active site of LSD1. Our aim was to achieve an analogous conformational restriction of a shorter peptide derived from the N-terminus of **1** by side-chain to side-chain macrocyclization as discussed above. After consideration of binding data obtained for the series of truncated peptides, Table 5, and the structure of **1** in complex with LSD1 we chose 11-meric peptide **4** as scaffold for design of macrocycles.

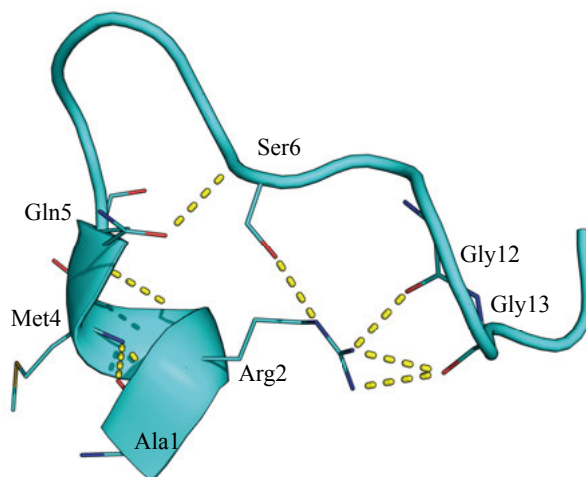


Figure 14. Secondary structure of pM4 (**1**) in the crystal structure with LSD1. The dotted yellow lines indicate intramolecular hydrogen bonds formed between residues in the N- and C-terminal parts of **1**. Key amino acids involved in intramolecular hydrogen bonding or binding to LSD1 have been labeled.

Table 6. Affinity data for binding of mono-substituted analogues of 11-meric peptide **6** to LSD1 determined by SPR.^a

Code	Sequence	aa ^x	K _D (μM)
4	ARTMQ TARKS T		140
7	PRTMQ TARKS T		10
8	Aaa ^x TMQ TARKS T	Cit	ND
9	ARTaa ^x Q TARKS T	Nle	>600
10	ARTaa ^x Q TARKS T	Aoc	>600
11	ARTaa ^x Q TARKS T	Homo-Phe	400
12	ARTMQ TAaa ^x KS T	Cit	ND

^aSubstitutions in aa^x: Cit: Citrulline, Nle: Norleucine; Aoc:(2S)-amino octanoic acid, homo-Phe:L-homophenylalanine.

We also set out to identify opportunities for modifications of side chains in the chosen scaffold **4** that contribute key binding interactions with LSD1. In particular, residues in **4** deduced to be important for complex formation by analysis of the crystal structures were investigated, i.e. Ala1, Arg2, Met4 and Arg8. Substitution of the cationic Arg2 and Arg8 with the polar but uncharged Cit (peptides **8** and **12**, Table 6) resulted in peptides binding below the detection limit, indicating that electrostatic interactions involving these residues are crucial for complex formation. Changing Met into more hydrophobic amino acids (cf. **9-11**, Table 6) did not increase the affinity. However, the hydrophobic pocket in LSD1 that accommodates Me4 appears sufficiently large to accommodate a bigger aromatic ring system, such as Homo-Phe.

2.3.4 Macrocycle synthesis

The rationale for preparation of macrocyclic peptides as inhibitors of LSD1 and general synthetic pathways to peptide macrocycles have been outlined briefly in Sections 1.3 and 2.3.2, respectively. The main focus here is to address the synthetic aspects of the cyclization step in greater detail. This is essential as macrocyclization is often the most difficult, and commonly the last step of the synthetic route. Failure, or low yields, in this step is therefore a concern that would require major adjustments of the synthetic strategy, or design of alternative cyclic peptides.

Table 7. Evaluation of catalysts for RCM to give 1-3 cyclic peptide II.

I	II
Catalyst	Estimated yield
Grubbs 1st	0
Grubbs 2nd	10 %
Hovda-Grubbs	15 %

a:DCM, room temperature, overnight. The reaction is performed with the peptide on solid phase, with all nucleophilic groups protected. The yields are estimated by the product peak intensity relative to that of the parent linear peptide in the reaction crudes by mass spectrometry.

Table 8. Optimization of conditions for RCM to give 1-3 cyclic peptide II.^a

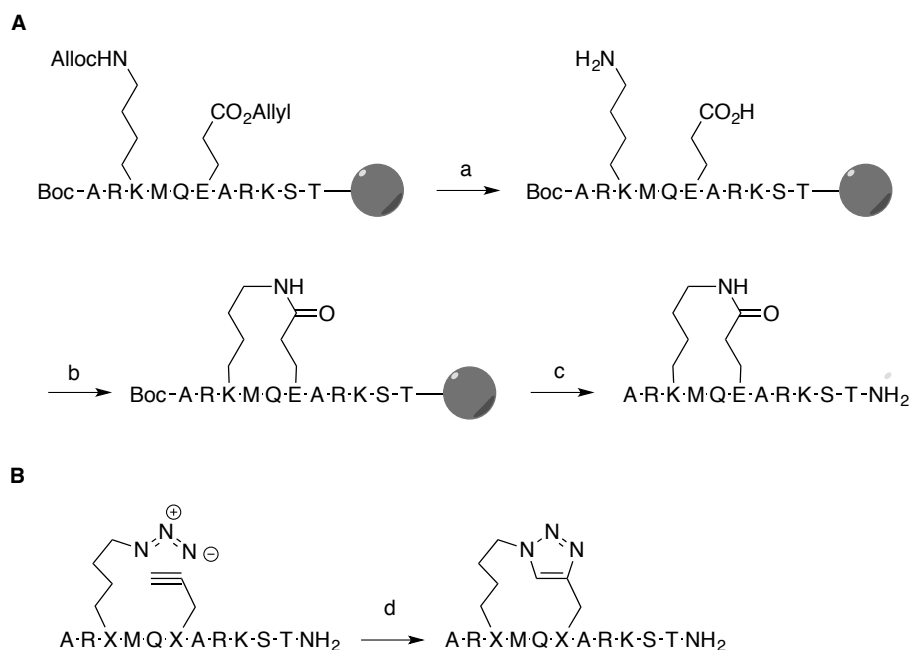
Temperature (°C)	Time (min)	Microwave	Estimated yield
50	5	yes	40 %
120	5	yes	60 %
200	5	yes	100 %
200	overnight	no	30 %

^aThe Hovda-Grubbs catalyst and DCB as solvent was used in all four reactions. Yields were estimated by mass spectrometry.

First, RCM (ring closing metathesis) was applied to synthesis of peptides olefin linkages between residues 1 and 3 or 3 and 6, respectively. Recently RCM has become the method of choice for peptide cyclization to give “stapled peptides”, which often display higher potency and cell permeability as compared to the linear parent. RCM is catalyzed by Grubbs (Ru IV) catalyst, of which there are several variants, and a multitude of applications reported in the literature.^{57,58,59} We investigated three different catalysts for

synthesis of the #1-3 cyclic peptides, Table 7, and obtained the best yield with the Hoveyda-Grubbs catalyst. However, we also found that the reaction conditions have a great impact and that the yield could be increased to 100 % when the temperature was increased to 200 °C by microwave irradiation, Table 8. Gratifyingly, the established reaction conditions were found to produce all of the other olefinic stapled peptides with 100 % conversion in the cyclization step.

Lactam and 1,2,3-triazole analogues of the most potent olefinic macrocyclic peptides were also prepared, Scheme 6. For the lactams the peptide was left on the solid phase, with Fmoc- and t-Bu protective groups intact, after completion of the automated synthesis. As alloc and allyl protective groups, which are orthogonal to Fmoc and t-Bu groups, had been used for lysine and glutamic acid at positions 3 and 6, they could be selectively deprotected under Pd (0) catalysis. Lactam formation was then achieved using HCTU as coupling reagent and DIPEA as base, followed by cleavage from the solid phase.



Scheme 6. Examples of cyclic peptides prepared by lactamization (A) and click chemistry (B). The triazole precursor was obtained by solid-phase synthesis, subsequently purified by RP-HPLC. *Reagents and Conditions:* a, N-methyl morpholine, Pd[P(Ph)₃]₄, acetic acid, 3 h; b, HCTU, N,N-diisopropylethylamine, DMF, 2 h; c, TFA, triethylsilane, water, 1,2-ethanedithiol and thioanisole (93:1:2.5:2.5:1), 1 h; d, CuSO₄, ascorbic acid, tert-BuOH/H₂O 1:2, 2 h, dark.

In contrast to cyclization by RCM and lactamization, 1,2,3-triazole formation was performed in solution phase as click chemistry is highly tolerant to the peptide functional groups. This relies on Cu(I) associating strongly with alkynes and azides, providing a catalytic core for 1,2,3-triazole formation. As the molecular weight does not change in the reaction it can not be monitored by MS alone. However, the cyclic products show distinct physicochemical properties and the cyclization can therefore be followed by RP-HPLC in combination with MS.

2.3.5 Evaluation of macrocyclic peptides

The set of stapled macrocyclic peptides was evaluated first in order to get insight into whether or not cyclization is a viable method for peptide inhibitor development, and what the desired spacer length might be, Table 9. Evaluation was performed by SPR in order to obtain direct binding data with high throughput. Then the impact of linkage chemo-type was investigated by comparison to lactam and triazole analogues of the most potent stapled peptides. Here, analysis was performed both by SPR and by determination of the inhibitory efficiency in an activity-based enzymatic assay.

Bridge length impacts on macrocycle affinity for LSD1

Table 9. Binding of stapled peptides and linear peptide precursors determined in a direct binding SPR assay.^a

Code	Sequence ^a	bridge atoms	K _D (μM)
4	ARTMQTARKST		140
7	PRTMQTARKST		10
13	G ^{aly} RG ^{aly} MQTARKST		26
14	<u>G</u> ^{aly} <u>R</u> G ^{aly} MQTARKST	4	NS ^b
15	ARG ^{aly} MQG ^{aly} ARKST		>100
16	AR <u>G</u> ^{aly} MQ <u>G</u> ^{aly} ARKST	4	>100
17	ARG ^{pen} MQG ^{pen} ARKST		NS ^b
18	AR <u>G</u> ^{pen} MQ <u>G</u> ^{pen} ARKST	8	15

^aThe underlined residues form the macrocyclic bridge. “G^{aly}” is L-allyl glycine, “G^{pen}” is L-pentenyl glycine. ^bNS indicates high non-specific binding.

According to our computational analysis, 4 to 6 carbon atoms are an optimal bridge length between the α-carbon atoms of residues 1 and 3, while 6 to 9 carbon atoms appear optimal for bridging positions 3 and 6, Figure 13. Interestingly, SPR showed that the binding affinity of 3-6 cyclized **18** is approximately 10 fold higher than that of the linear H3-derived peptide **4**, table 9.

The binding characteristics of **18** is also distinct from its linear precursor **17**, which shows high non-specific binding. It is likely that the eight carbon atom bridge of **18** has restrained the peptide conformation to an active one and that the affinity is increased by entropic penalty compensation by the bridge. At the same paired positions, **16** has a shorter bridge than that suggested to be optimal by modeling. Peptide **16** and its linear precursor **15** bind to LSD1 with an affinity comparable to that of H3 peptide **4**, supporting that cyclization and bridge length are important for binding. Modeling also suggested that four carbon atoms would be optimal for bridging positions 1 and 3. However, at this position modeling did not agree with the experimental results as cyclic **14** showed high non-specific binding. In contrast, the linear precursor **13** was a potent binder, just as **7** which has proline at position 1. Very likely, additional hydrophobic contacts made by the allyl side chain at position 1 in **13**, and proline in **7**, may well explain their increased affinity for LSD1.

Linkage chemo-type impacts on macrocycle affinity for LSD1

Table 10. Inhibition data for macrocycles determined by activity-based assay.^a

Code	Sequence ^a	bridge atoms	K _i (μM)	Residual activity (%) ^b
4	ARTMQTARKST		>100	>80
18	AR <u>G</u> ^{pen} MQ <u>G</u> ^{pen} ARKST	Staple	IC ₅₀ 15	25
19	AR* <u>G</u> ^{pen} MQ <u>G</u> ^{pen} ARKST	Staple	8.5 (IC ₅₀ 11)	5
20	AR <u>G</u> ^{pen} MQ* <u>G</u> ^{pen} ARKST	Staple	IC ₅₀ 6	5
21	AR* <u>G</u> ^{pen} MQ* <u>G</u> ^{pe} nARKST	Staple	IC ₅₀ 5	10
22	AR <u>K</u> MQEARKST	Amide	31	35
23	AR* <u>K</u> MQEARKST	Amide	2.3	<1
24	AREMQ <u>K</u> ARKST	Amide	4	2
25	AR* <u>E</u> MQKARKST	Amide	>100	>80
26	PR <u>K</u> MQEARKST	Amide	7	10
27	PREMQ <u>K</u> ARKST	Amide	22	25
28	AR <u>K</u> ^{azd} MQ <u>G</u> ^{prg} ARKST	Triazole	>75	>70
29	AR <u>G</u> ^{prg} MQ <u>K</u> ^{azd} ARKST	Triazole	30	30

^aThe underlined residues form the macrocyclic bridge. “G^{aly}” is L-allyl glycine, “G^{pen}” is L-pentenyl glycine, “*G^{pen}” is D-pentenyl glycine, “*K” is D-lysine, “*E” is D-glutamic acid, “K^{azd}” is L-5-azido lysine, “G^{prg}” is L-progargyl glycine. ^bv_i/v₀ for [I]=100 μM. The residual activity calculated after 3 min from initiation of the reaction.

Evaluation of the stapled peptides indicated that an eight carbon atom bridge between residues 3 and 6 constrains the peptide conformation closer to the

bioactive one. Macrocycles **19-29** having other types of linkages were used to further explore opportunities for better inhibitors. Compounds **19-21** are stapled peptides with different stereochemical properties at the linkage residues, which have almost identical inhibitory activities in the activity-based enzymatic assay. In contrast to lactams **22-25** and 1,2,3-triazoles **26-27**, the stapled peptides do not behave as competitive inhibitors, with the exception of **19**. Lactam **23** was found to be the best inhibitor with a K_i of 2.3 μM , which constitutes >43 fold increase in inhibitory activity as compared to reference peptide **4**. We suggest that the amide linkage has contributed additional binding affinity for LSD1, and/or an even more optimal conformation. The 1,2,3-triazole linkage is assumed to be quasi-isosteric to a lactam bridge, and the lower potency of **28-29** as compared to the lactams therefore indicate that the bridge of the latter may participate in hydrogen bonding with LSD1. Lactams **26** and **27** were prepared with the hope of gaining synergistic inhibitory potency from the N-terminal proline and the lactam bridge. Unfortunately, this expectation was not fulfilled.

Summary

LSD1 is an intracellular enzyme that selectively catalyzes the demethylation reaction of histone 3 methylated on the Lys4 and Lys9. It functions as an epigenetic regulator of gene expression and has been associated with various types of cancer. Thereby LSD1 is a therapeutically interesting target for design of novel oncology drugs. In this paper we have developed macrocyclic peptides as inhibitors of LSD1 based on co-crystal structures of the enzyme with peptides derived from the histone 3. The side chains between residues 1-3 or 3-6 were connected by cyclization, but only 3-6 bridged macrocycles were potent binders of LSD1. At this position we found that eight carbon atoms are optimal to constrain the peptide in an active conformation and that lactam linkages provided more potent inhibitors of LSD1 than stapled and 1,2,3-triazole based linkages. An activity-based assay revealed lactam **23** to be the most potent competitive inhibitor of LSD1, with a K_i of 2.3 μM . Its activity is thus >40 fold higher than that of the linear H3 peptide of the same length. Because the peptide sequence originates from H3, it is likely that **23** is a selective inhibitor of LSD1. In addition, it also provides a scaffold for design of novel peptidomimetic drugs; an objective that would benefit from determination of the crystal structure of the complex between **23** and LSD1.

Conclusion and Outlook

The overall aim of my thesis is to develop high affinity binders using a combination of organic and peptide chemistry. This aim was pursued in three related projects.

Based on the results from a fragment screen the small organic molecule DQ was designed to recognize CRP in a Ca^{2+} independent manner. The binding characteristic of DQ was entailed on the polypeptide conjugate, 4-C25L22-DQ. Additionally, the affinity was increased by at least three orders of magnitudes by the attached peptide scaffold. The design of CRP binder, 4-C25L22-DQ, illustrates that the small organic molecules used in the peptide binder concept are not limited to naturally occurring ligands or known inhibitors for protein receptors. Instead, low affinity ligands may be discovered by techniques used in the early stages of drug discovery, and then rapidly transformed into binders having high affinity and selectivity. Thus, the toolbox available for development of protein binders has been enlarged.

The polypeptide conjugate 4-C10L17-AZM was developed to recognize HCA II and HCA IX with affinities that are larger than the small molecule ligand AZM. Most encouragingly, 4-C10L17-AZM was found to bind HCA II and IX with dissociation constants of 4 nM and 90 pM, respectively, i.e. 10- and 33-fold better than AZM. Most likely 4-C10L17-AZM binds HCA IX more strongly than HCA II due to interactions with the proteoglycan domain, which is only present in HCA IX. Thus, development of 4-C10L17-AZM constitutes proof of concept that the binder strategy is able to provide recognition elements with dissociation constants in the pM range.

A cyclization strategy inspired by structure-based design was applied to find potent inhibitors of LSD1, an epigenetic enzyme implicated in development of cancer. Cyclic peptides with tethers between the side chains of residues 3 and 6, in general, displayed higher affinity binding than the original linear parent peptide. Among the three series evaluated, lactam cyclic peptides were found to be the best inhibitors of LSD1, with potencies ranging from a K_i of 2 μM and upward. The discovered lactam scaffold is therefore of interest in efforts to generate peptidomimetic drugs that inhibit LSD1. Such efforts would benefit significantly from determination of the structure of a complex between a lactam and LSD1.

Methods

3.1 Peptide synthesis

Solid phase peptide synthesis (SPPS), developed by Bruce Merrifield in 1963, is the method of choice for chemical synthesis of peptides.⁶⁰ The advantage of SPPS is that a cycle of coupling and washing steps are used for stepwise elongation of a peptide chain starting from the C-terminal amino acid attached covalently to resin beads, Figure 15. Thus no purifications are needed until the peptide is cleaved from the solid phase. Nucleophilic groups of each amino acid are protected with a temporary protecting group on N^α and semi-permanent protecting groups on side chains.

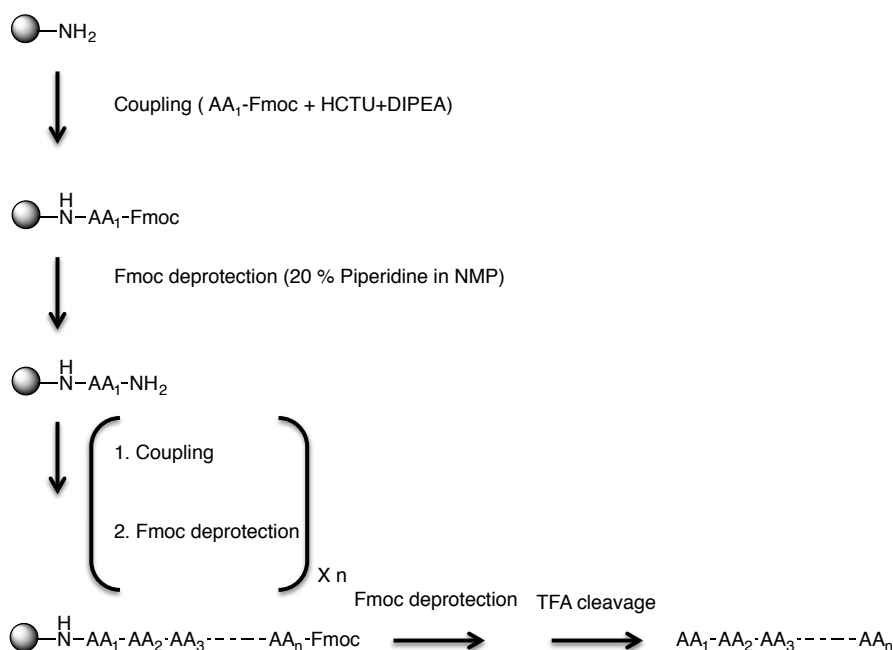


Figure 15. SPPS is initiated by removal of the temporary protecting group from N^α of the C-terminal amino acid, which is covalently linked to the solid support. The carboxyl group of the second amino acid is activated in solution and then reacted with the N^α-amino group to form an amide bond. These reactions are then repeated for further elongation of the peptide to the desired length. Finally, the semi-permanent protecting groups are removed at the same time as the peptide is cleaved from the solid support.

Two different strategies are in common use for SPPS. The Boc-/Benzyl strategy uses the Boc group as a temporary protecting group at the N^α-amino groups and benzyl or Cbz (carboxybenzyl) groups as semi-permanent protecting groups for the side-chains. Boc groups are deprotected with TFA and the peptide is cleaved from the solid support with anhydrous hydrogen fluoride (HF). The Fmoc/t-Butyl strategy is another and milder strategy for SPPS. Here, the temporary Fmoc protective group is removed by the mild base piperidine, while the final deprotection of t-Butyl and Boc groups is performed with TFA simultaneously with cleavage of the peptide from the solid phase. Because deprotections are much milder than in the Boc-/Benzyl strategy, the Fmoc/t-Butyl approach has become the more commonly used method for SPPS.

3.2 NMR spectroscopy

3.2.1 WaterLOGSY

In the recent decades, NMR spectroscopy has emerged as a screening method to identify small molecules that bind to protein drug targets.⁶¹ On the basis of detecting mechanism of resonances, the method has been subclassed into ligand-observed and receptor (macromolecular targets)-observed spectroscopic strategy. WaterLOGSY belongs to the first class and was developed on the basis of magnetization transfer from bulk water. Merits that justify the introduction of this type of method for screening is that less protein and ligand material is required for good sensitivity. With a selective pulse that saturates the water resonance, magnetization from bulk water is transferred to other molecules provided that the ligand molecule is complexed with its protein receptor.⁶² The magnetization from bulk water will be transferred to the free ligand molecules in solution as well as to the ones bound to the receptors. Because bulk water molecules surround the free ligands, the resonance of free ligand is saturated due to the effect and hence no signal from them will show in the ¹H NMR spectrum. In contrast, the resonance from the bound ligand remains since they are buried in the pocket of the receptor and separated from the bulk water. The ligand proton resonance associated with binding to the receptor is then characterized from the observation of the ¹H NMR spectrum of the small molecule.

The advantage of this method is that it is possible to identify binding of several small molecules simultaneously in a solution with a protein receptor. In paper I, an 18-membered set of fragments was screened using the WaterLOGSY experiment and three fragment molecules (**1,2,3**) that interact with CRP were identified, Figure 16. The affinity of each molecule was not quantitatively measured, whereas the information obtained from the WaterLOGSY experiment was enough to identify the lead fragments. It was a key

finding that the binding fragments did not require the presence of Ca^{2+} . The experiment was carried out in a Ca^{2+} free environment. Consequently, the calcium independent interactions of the lead fragments were expected to hold also for the peptide conjugate binder.

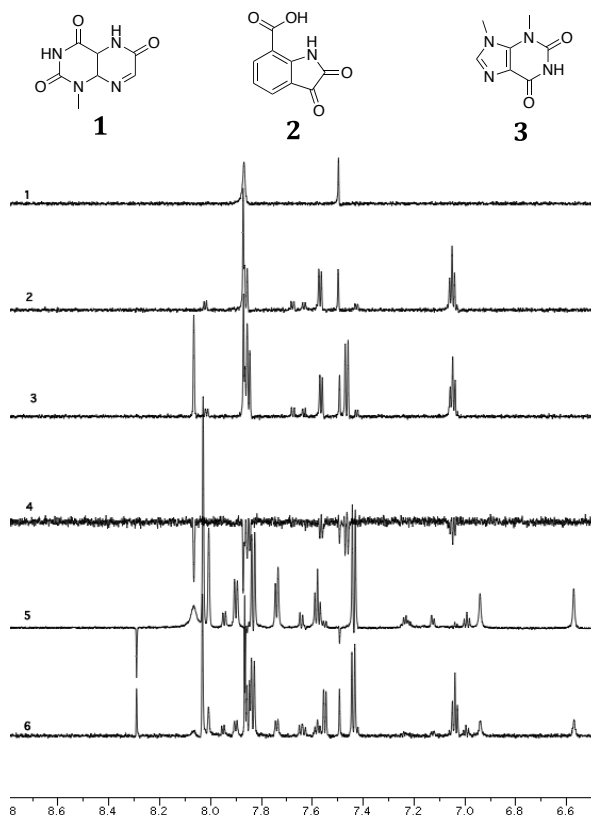


Figure 16. WaterLOGSY experiment revealing binding of compounds **1**, **2** and **3** for CRP. Protein concentration was 7 μM in PBS buffer. Spectrum 1 is **3**, spectrum 2 is **2** and **3**, spectrum 3 is **1**, **2** and **3**. Spectrum 4 is waterLOGSY experiment showing inverted peaks of **1**, **2** and **3** due to interaction with CRP. Spectrum 5 shows waterLOGSY control experiment of **1**, **2**, **3** and two other control compounds where inversion of a few protons is observed. Spectrum 6 is ^1H NMR of the compound mix.

3.3.2 2D Spectroscopy for peptide structural analysis

The chemical shifts of protons play an essential role in determination of molecular structure. But in the cases of peptides and proteins, the signals are not well dispersed. Two-dimensional (2D) NMR spectroscopy is often used to resolve the overlap of signals. Secondary structures for instance, helices and beta-sheets, can be predicted based on the deviation of residue chemical shifts (^1H , ^{13}C , ^{15}N) from those in an unordered biopolymer.⁶³⁻⁶⁶ 2D spectra also provide information about scalar couplings (coupling through covalent

bond) and dipole-dipole couplings (NOE) that combined with chemical shifts can be used to calculate 3 dimensional structures.

In order to determine peptide structures, initially protons are assigned to each amino residue. This task is easier when the peptide sequence is known, and the primary structure can be verified by inter-residue NOE signals. Even if the sequence is unknown, it can be determined by the analysis of NOESY spectra.

The cross peak integrals of NOESY spectra provide information about whether the protons are close in space. The calibration of the cross peak integrals with those of a known reference (e.g. germinal protons) converts the cross peak volume into interproton distances. The internuclear distances, $d(H^{\alpha}, H^N)$, $d(H^N, H^N)$, $d(H^{\beta}, H^N)$, are also dependent on the torsion angles of the peptide backbone and hence the cross peak integrals of NOESY spectra can also provide torsion angle information. The compiled information is then used to compute the peptide structure.

3.3 Fluorescence spectroscopy

Fluorescence spectroscopy is commonly used to study binding interactions e.g. in protein folding, protein ligand binding and macromolecular recognition. A handful of compounds that are sensitive to environmental changes (e.g. hydrophobicity, pH, energy transfer, anisotropy) are routinely used to study molecular interactions.⁶⁷ It is critical to choose the optimal fluorophore for each interaction and the incorporation site is also very important. In the development of a peptide based biosensor for antibody fragment detection Enander et al attempted to attach the fluorophore to two different sites of the peptide construct. The one with the probe at C-terminal, which is seven amino acid residues away from the site of incorporation of the small molecule residue showed 40% emission intensity change upon peptide binding. When the probe was two amino residues away, no change in fluorescence was observed.⁶⁸ A similar study was carried out by Choulier in an antigen-antibody system. With respect to the position of the fluorescent tag in the peptide sequence incorporation at the side chain of the residue zero, two and five amino acids away from the binding epitope, only one sensed the peptide antigen-antibody interaction. The addition of the antibody to a solution of the peptide with the probe two amino residues distant from the epitope, decreased the intensity of the emitted light.⁶⁹ Presumably, the site of incorporation of the fluorophore is also important in the designed polypeptides. 7-Methoxycoumarin is sensitive to a change in polarity of the surrounding medium and was routinely incorporated at polypeptide lysyl side chains for titration purposes. On the same face of the presumed amphiphilic helix, a second lysine was incorporated for the introduction of a ligand molecule, Figure 17. In the putative structure, both fluorophore (coumarin) and ligand

are projected on the same topological face, allowing reporters to sense a similar environmental change as that of the ligand molecule upon association with the protein.

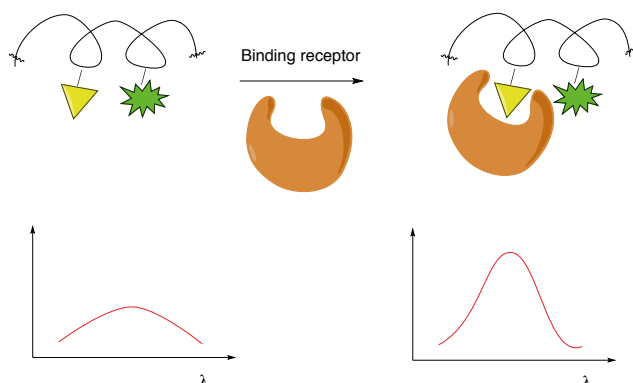


Figure 17. Principle of coumarin disclosing the binding between the peptide conjugate and protein receptor. The emission light has increased by addition of protein receptor to peptide conjugate.

The equilibrium dissociation constant K_d can be determined from the hyperbolic binding curves obtained upon titration of the peptide conjugate with the protein. However, a titration in 3 steps is an efficient way to screen the relative affinities of 16 polypeptide conjugates, and approximate affinities can still be obtained. In Paper I, 4-C25L22-DQ was estimated to have an affinity value in the range of 200-500 nM from fluorescence screening, a value that is close to that accurately measured by SPR.

3.4 Surface Plasmon Resonance

Surface plasmon resonance (SPR) is an increasingly popular label-free technology that is appreciated for its high sensitivity and unusually information-rich output. Essentially, the target molecule (receptor, P) is immobilized on a dextran-coated sensor chip, and a solution containing the binding counterpart (ligand, B) is flowed over the sensor chip. On the opposite side of the chip surface, a light beam is scattered to the sensor chip surface and the reflected light is detected. A sensorgram describing the interaction of the ligand with the immobilized receptor is generated from the light angle change induced by complex formation. The response (R) is proportional to the amount of formed complex, [PB] and the sensorgram directly presents the association and dissociation of ligand in real time. The theoretical aspects of how rate and equilibrium binding constants are derived from the SPR sensorgram are described in the following sections.

Affinity determination by fitting with kinetic equation⁷⁰

Provided that the receptor and analyte are in a 1:1 reversible binding relationship in the association phase, the complex $[PB]$ increases as a function of time according to

$$\frac{d[PB]}{dt} = k_a[P][B] - k_d[PB] , \quad \text{Eq. 2}$$

where k_a is the association rate constant and k_d is the dissociation rate constant. After a certain time, t , $[P]=[P]_0-[PB]$. Substituting into Eq. 2 gives

$$\frac{d[PB]}{dt} = k_a[B]([P]_0 - [PB]) - k_d[PB] . \quad \text{Eq. 3}$$

As was previously mentioned, the signal observed, R , is proportional to the formation of the PB complex, and thence maximum signal, R_{max} , will be proportional to the maximum amount of PB complex. Equation 3 then becomes

$$\frac{dR}{dt} = k_a C(R_{max} - R) - k_d R . \quad \text{Eq. 4}$$

Integration of Eq. 4 gives

$$R_t = \frac{Ck_a R_{max} [1 - e^{-((Ck_a + k_d)t)]}}{Ck_a + k_d} . \quad \text{Eq. 5}$$

In the dissociation phase, the complex $[PB]$ decreases as a function of time according to

$$\frac{d[PB]}{dt} = -k_d[PB] . \quad \text{Eq. 6}$$

After same procedure, Eq. 6 can be rewritten and integrated into

$$R_t = R_a e^{-k_d t} , \quad \text{Eq. 7}$$

where R_a is defined as the amplitude of the dissociation process.

The rate constants are extrapolated by fitting Eq. 4 and 6 to the sensor-gram on the binding association and dissociation phases, respectively. The dissociation constant is then provided by inputting k_a , k_d into

$$K_D = k_d / k_a . \quad \text{Eq. 8}$$

Affinity determination by fitting with steady-state equation

At steady state, $\frac{dR}{dt}$ equals 0 and thence Eq. 4 can be written as

$$R = \frac{C R_{max}}{K_D + 1} , \quad \text{Eq. 9}$$

where R is response which is dependent on the concentration of the ligand. In order to determine the K_D , it is suggested to obtain R from at least five different concentrations in the range of approximate K_D .

Svensk sammanfattning

Denna avhandling beskriver undersökningar av två koncept för affinitetshöjning av proteinbindare. Det första konceptet bygger på att man kan förstärka affiniteten hos en proteinbindande molekyl ("liganden") genom koppling (konjugering) till en speciell sorts peptider. Detta koncept har använts för utveckling av högaffinitetsbindare till proteinerna CRP (C-Reactive Protein) och HCA (Human Carbonic Anhydrase). Det andra konceptet bygger på att framställa en ringformig förening (makrocycl) genom cyklisering av en peptidsekvens som man vet binder till ett protein. I detta fall har konceptet använts för utveckling av bindare till enzymet LSD1.

CRP är ett protein vars serumkoncentration ökar vid många sjukdomstillstånd, och CRP-bestämning används därför ofta inom medicinsk diagnostik. Därför utvecklades ett högaffinitets-peptidkonjugat (4-C25L22-DQ) för specifik CRP-igenkänning och möjlig användning för diagnostik. Liganden (DQ) utformades utifrån strukturerna hos tre molekyler (av 18 undersökta) som vid NMR-experiment visat sig binda till CRP med mätbar affinitet. Liganden syntetiserades i form av sin aktiva ester, som sedan konjugerades till fyra peptider från ett peptidbibliotek. Konjugatens affinitet till CRP utvärderades med fluorescensspektroskopi, varvid två (4-C15L8-DQ och 4-C25L22-DQ) visade hög affinitet. För konjugatet 4-C25L22-DQ gjordes ytterligare affinitetsmätningar med ytplasmonresonans (SPR). Dissociationskonstanten för bindning till CRP uppmättes till 330 nM i närvaro av Ca^{2+} joner och till endast obetydligt högre i frånvaro av Ca^{2+} , vilket visade att bindningen mellan 4-C25L22-DQ och CRP inte kräver närvaro av Ca^{2+} . Därför borde konjugatet 4-C25L22-DQ kunna fungera som ett CRP-diagnostikverktyg även vid låga Ca^{2+} -koncentrationer. Vi kunde också visa att immobiliserad 4-C25L22-DQ kunde selektera ut CRP ur humant serum. Bindningsexperiment i närvaro av en känd CRP-bindare (fosforylkolin) visade att DQ-liganden inte binder till samma plats på CRP-proteinets yta som fosforylkolin.

HCA IX är ett protein som är intressant inom cancerdiagnostik. Det är känt att HCA-proteiner binder till flera olika mindre molekyler, t.ex. acetazolamid. Ett acetazolamidderivat (AZM) med en 10-atoms "spacer" utformad för konjugering framställdes och konjugerades till ett antal peptider med nettoladdningar på mellan +2 och -5. SPR-experiment visade att konjugatet 4-C10L17-AZM hade den lägsta dissociationskonstanten, vilket innebär en tiofaldig affinitetsökning för HCA II jämfört med okonjugerad

acetazolamid. Vi kunde också visa att bindningen mellan 4-C10L17-AZM och HCA II upphävdes i närvaro av acetazolamid. Konjugatet 4-C10L17-AZM binder med ännu högre affinitet (dissociationskonstant 90 pM) till proteinet HCA IX, medan affiniteten till HCA IX-varianter som saknar en s.k. PG-domän inte skilde sig nämnvärt från okonjugerad acetazolamid. Detta beror troligen på att affinitetsökningen vid konjugering av acetazolamid till peptid beror på en interaktion mellan konjugatets peptidkomponent och HCA-proteinets PG-domän.

Proteinet HCA IX förekommer rikligt i vissa tumörceller och konjugatet 4-C10L17-AZM är därför ett tänkbart verktyg för påvisandet av denna cancermarkör. Andra, mindre molekyler som hittills använts för detta ändamål kan inte skilja mellan HCA IX och HCA I/HCA II (de senare förekommer rikligt i alla celler). Konjugatet 4-C10L17-AZM uppvisade en dissociationskonstant på 90 pM gentemot HCA IX jämfört med 4 nM för HCA II, så man kan förvänta sig en högre specificitet än för de andra mindre molekyler. Konjugatet är därför högtintressant som verktyg vid tumöravbildning eller vid annan medicinsk diagnostik baserad på HCA IX som cancermarkör.

LSD1 är ett enzym som katalyserar N-demetylering av metylerat histoneprotein (H3). Denna demetylering påverkar aktivering av vissa gener, och man har visat att vissa substanser som hämmar, dvs binder till, LSD1-enzymet kanske kan användas som cancerläkemedel. Denna avhandling beskriver utformning och framställning av makrocycliska peptider med utgångspunkt från en peptidsekvens (pM4) i H3-proteinet som man vet är inblandad i bindningen till LSD1-enzymet. Cyklisering genom ”bryggning” mellan olika aminosyror och funktionella grupper i den linjära peptiden utfördes, och ett antal kandidater med mätbar bindning till LSD1 identifierades med hjälp av SPR och enzymaktivitets-mätningar. Bäst var den cykliska föreningen 23, som var en kompetitiv inhibitor av LSD1 med en $K_i = 2.3 \text{ microM}$, vilket är 43-faldigt bättre än motsvarande icke-cykliska struktur. Strukturanalys visade att förening 23 tenderar att anta helix-form i den N-terminala regionen. En interaktion mellan en amidgrupp och laktambryggan i 23 observerades också. Denna interaktion kan antas tvinga peptiden 23 att anta en form som binder starkt till LSD1-enzymet. Eftersom 23 har sitt ursprung i en LSD1-bindande H3-peptidsekvens är det också sannolikt att bindningen är mycket specifik för just LSD1, vilket är viktigt för dess användbarhet som läkemedel. Förening 23 kan också, under förutsättning att kristallstrukturen hos enzym-23-komplexet kan erhållas, tjäna som utgångspunkt för vidare design av cancer-läkemedelkandidater.

Acknowledgement

Foremost, I would like to express my sincere gratitude to my two main advisors Prof. Jan Khilberg and Prof. Lars Baltzer for the continuous support of my Ph.D. study and research, for your patience, motivation, enthusiasm, and immense knowledge. Having research projects as well as writing of this thesis becomes very enjoyable under your supervision.

Besides my advisors, I would like to thank Prof. Thomas Norberg for leading me in the organic synthesis. It is always fun to discuss chemistry with you. I could not wait to having next boat trip with you and Aleksandra, it was one of my best moments in Sweden.

I want to acknowledge Prof. Adolf Gogoll and Prof. Helena Grennberg for your helps during my Ph.D. study.

My sincere thanks also go to Dr. Johan Viljanen by leading me in the peptide chemistry, and sharing your practical experiences, which are precious to me.

Aleksandra Balliu, as my best friend and my colleague, you have become Doctor when you read this. I want to thank your for you support during my Ph.D., and wish you a good fortune in the coming carrier.

I thank my fellow labmates in LB Group: Susanna, and in JKG group: Nathan, Mohit, Lina, Fabio and Stefan for the stimulating discussions, for proof reading of my thesis in two days and for all the fun we have had in these years. Especially to Nathan, you make me understand the science is also a beautiful art, and I am grateful for helping me design the front page for my thesis.

I want to acknowledge my collaborators Prof. Helena Danielson and Ph.D. student Vladimir for your best efforts in LSD1 project, as well as the insightful discussions.

Last but not the least, I would like to thank my family: my parents Qishun Yang and Yuhu Huang, for giving birth to me at the first place and supporting me spiritually throughout my life. My wife, Yu Qi, thank you to always accompany with me, encourage me and bring me so much happiness.

References

1. Huston, J. S.; George, A. J. T. *Hum. Antibodies*, **2001**, *10*, 127–142.
2. Stumpp, M. T.; Amstutz, P. *Curr Opin Drug Discov Devel.*, **2007**, *10*, 153–159.
3. Feldwisch, J.; Tolmachev, V.; Lendel, C.; Herne, N.; Sjöberg, A.; Larsson, B.; Rosik, D.; Lindqvist, E.; Fant, G.; Höidén-Guthenberg, I.; Galli, J.; Jonasson, P.; Abrahmsén, L. *J. Mol. Biol.*, **2010**, *398*, 232–247.
4. Schönfeld, D.; Matschiner, G.; Chatwell, L.; Trentmann, S.; Gille, H.; Hülsmeier, M.; Brown, N.; Kaye, P. M.; Schlehuber, S.; Hohlbaum, A. M.; Skerra, A. *Proc. Natl. Acad. Sci. U.S.A.*, **2009**, *106*, 8198–8203.
5. Lipinski, C. A.; Lombardo, F.; Dominy, B. W.; Feeney, P. J. *Adv. Drug Deli. Rev.* **2001**, *46*, 3–26.
6. Driggers, E. M.; Hale, S. P.; Lee, J.; Terrett, N. K. *Nat. Rev. Drug Discov.*, **2008**, *7* (7), 608–624.
7. Hruby, V. J. *Nat. Rev. Drug Discov.*, **2002**, *1* (11), 847–858.
8. Scott, D. E.; Bayly, A. R.; Abell, C.; Skidmore, J. *Nat. Rev. Drug Discov.*, **2016**, *15*, 533–550.
9. Grabowski, S. J. *Hydrogen bonding: new insights*; **2006**. Dordrecht: Springer.
10. Grabowski, S. J. *Chem. Rev.*, **2011**, *111*, 2597–2625.
11. Steiner, T. *Angew. Chem. Int. Ed. Engl.* **2002**, *41*, 48–76.
12. Ludwig, R. *Angew. Chem. Int. Ed. Engl.* **2001**, *40*, 1808–1827.
13. Jencks, W. P. *Proc. Natl. Acad. Sci. U.S.A.*, **1981**, *78*, 4046–4050.
14. Olofsson, S.; Johansson, G.; Baltzer, L. *J. Chem. Soc., Perkin Trans. 2*, **1995**, *0*, 2047–2056.
15. Andersson, T.; Lundquist, M.; Dolphin, G. T.; Enander, K.; Jonsson, B.-H.; Nilsson, J. W.; Baltzer, L. *Chem. Biol.*, **2005**, *12*, 1245–1252.
16. Tegler, L. T.; Nonglaton, G.; Büttner, F.; Caldwell, K.; Christopeit, T.; Danielson, U. H.; Fromell, K.; Gossas, T.; Larsson, A.; Longati, P.; Norberg, T.; Ramapanicker, R.; Rydberg, J.; Baltzer, L. *Angew. Chem. Int. Ed. Engl.*, **2011**, *50*, 1823–1827.
17. Baltzer, L. *Anal. Bioanal. Chem.*, **2011**, *400*, 1653–1664.
18. Tegler, L.T. *Polypeptide Conjugates as High-Affinity Binders for Proteins*. Acta Universitatis Upsaliensis, **2009**.
19. Smith, M. C.; Gestwicki, J. E. *Expert. Rev. Mol Med.*, **2012**, *14*, 481.
20. Sheinerman, F. B.; Norel, R.; Honig, B. *Curr. Opin. Struct. Biol.* **2000**, *10*, 153–159.
21. Balliu, A.; Baltzer, L. *ChemBioChem* **2017**, *14*, 1.
22. Morgan, B. A.; Gainor, J. A. *Annu. Rep. Med. Chem.*, **1989**, *24*, 243–252.
23. Giannis, A.; Kolter, T. *Angew. Chem. Int. Ed. Engl.* **1993**, *32*, 1244–1267.
24. Gante, J. *Angew. Chem. Int. Ed. Engl.*, **1994**, *33*, 1699–1720.
25. Hill, T. A.; Shepherd, N. E.; Diness, F.; Fairlie, D. P. *Angew. Chem. Int. Ed. Engl.*, **2014**, *53*, 13020–13041.

26. Dupuy, A. M.; Terrier, N.; Senecal, L.; Morena, M.; Leray, H.; Canaud, B.; Cristol, J. P. *Nephrologie*, **2003**, *24*, 337–341.
27. Enander, K.; Dolphin, G. T.; Baltzer, L. *J. Am. Chem. Soc.* **2004**, *126*, 4464–4465.
28. Tegler, L. T.; Fromell, K.; Jonsson, B.-H.; Viljanen, J.; Winander, C.; Carlsson, J.; Baltzer, L. *ChemBioChem.*, **2011**, *12*, 559–566.
29. Ramapanicker, R.; Sun, X.; Viljanen, J.; Baltzer, L. *Bioconjug. Chem.*, **2013**, *24*, 17–25.
30. Sun, X.; Yang, J.; Norberg, T.; Baltzer, L. *J. Pept. Sci.*, **2012**, *18*, 731–739.
31. Mark B Pepys, G. M. H. *J. Clin. Invest.*, **2003**, *111*, 1805–1812.
32. Srikantiah, C. *IJRCI*, **2014**, *2*, 1–24.
33. Tominaga, M.; YO, E.; Ogawa, H.; Yamashita, S.; Yabuuchi, Y.; Nakagawa, K. *Chem. Pharm. Bull.*, **1986**, *34*, 682–693.
34. Thompson, D.; Pepys, M. B.; Wood, S. P. *Structure*, **1999**, *7*, 169–177.
35. Lou, Y.; McDonald, P. C.; Oloumi, A.; Chia, S.; Ostlund, C.; Ahmadi, A.; Kyle, A.; Keller, U. A. D.; Leung, S.; Huntsman, D.; Clarke, B.; Sutherland, B. W.; Waterhouse, D.; Bally, M.; Roskelley, C.; Overall, C. M.; Minchinton, A.; Pacchiano, F.; Carta, F.; Scozzafava, A.; Touisni, N.; Winum, J.-Y.; Supuran, C. T.; Dedhar, S. *Cancer Res.*, **2011**, *71*, 3364–3376.
36. Ward, C.; Meehan, J.; Mullen, P.; Supuran, C.; Dixon, J. M.; Thomas, J. S.; Winum, J.-Y.; Lambin, P.; Dubois, L.; Pavathaneni, N.-K.; Jarman, E. J.; Renshaw, L.; Um, I.; Kay, C.; Harrison, D. J.; Kunkler, I. H.; Langdon, S. P. *Oncotarget* **2015**, *6*, 24856–24870.
37. Köhler, K.; Hillebrecht, A.; Schulze Wischeler, J.; Innocenti, A.; Heine, A.; Supuran, C. T.; Klebe, G. *Angew. Chem. Int. Ed. Engl.*, **2007**, *46*, 7697–7699.
38. GE Health. Biacore Concentration Analysis Handbook. **2001**. Retrieved from <https://www.biacore.com/lifesciences/service.downloads/Handbooks/index.html?section=lifescience&realsection=lifesciences>.
39. Konovalov, S.; Garcia-Bassets, I. *J. Ovarian. Res.*, **2013**, *6*, 75.
40. Zang, C.; Nie, F.-Q.; Wang, Q.; Sun, M.; Li, W.; He, J.; Zhang, M.; Lu, K.-H. *Oncotarget*, **2016**, *7*, 11696–11707.
41. Serce, N.; Gnatzy, A.; Steiner, S.; Lorenzen, H.; Kirfel, J.; Buettner, R. *BMC Clin Pathol*, **2012**, *12*, 13.
42. Zhao, Z.-K.; Yu, H.-F.; Wang, D.-R.; Dong, P.; Chen, L.; Wu, W.-G.; Ding, W.-J.; Liu, Y.-B. *World J. Gastroenterol.*, **2012**, *18*, 6651–6656.
43. McAllister, T. E.; England, K. S.; Hopkinson, R. J.; Brennan, P. E.; Kawamura, A.; Schofield, C. J. *J. Med. Chem.*, **2016**, *59*, 1308–1329.
44. Ogasawara, D.; Suzuki, T.; Mino, K.; Ueda, R.; Khan, M. N. A.; Matsubara, T.; Koseki, K.; Hasegawa, M.; Sasaki, R.; Nakagawa, H.; Mizukami, T.; Miyata, N. *Bioorganic. Med. Chem.*, **2011**, *19*, 3702–3708.
45. Vianello, P.; Botrugno, O. A.; Cappa, A.; Ciossani, G.; Dessanti, P.; Mai, A.; Mattevi, A.; Meroni, G.; Minucci, S.; Thaler, F.; Tortorici, M.; Trifirò, P.; Valente, S.; Villa, M.; Varasi, M.; Mercurio, C. *Eur. J. Med. Chem.*, **2014**, *86*, 352–363.
46. Nakayama, S.; Atsumi, R.; Takakusa, H.; Kobayashi, Y.; Kurihara, A.; Nagai, Y.; Nakai, D.; Okazaki, O. *Drug Metab. Dispos.* **2009**, *37*, 1970–1977.
47. Nowotarski, S. L.; Pachaiyappan, B.; Holshouser, S. L.; Kutz, C. J.; Li, Y.; Huang, Y.; Sharma, S. K.; Casero, R. A.; Woster, P. M. *Bioorganic. Med. Chem.*, **2015**, *23*, 1601–1612.

48. Ma, L.-Y.; Zheng, Y.-C.; Wang, S.-Q.; Wang, B.; Wang, Z.-R.; Pang, L.-P.; Zhang, M.; Wang, J.-W.; Ding, L.; Li, J.; Wang, C.; Hu, B.; Liu, Y.; Zhang, X.-D.; Wang, J.-J.; Wang, Z.-J.; Zhao, W.; Liu, H.-M. *J. Med. Chem.*, **2015**, *58*, 1705–1716.
49. Zheng, Y.-C.; Duan, Y.-C.; Ma, J.-L.; Xu, R.-M.; Zi, X.; Lv, W.-L.; Wang, M.-M.; Ye, X.-W.; Zhu, S.; Mobley, D.; Zhu, Y.-Y.; Wang, J.-W.; Li, J.-F.; Wang, Z.-R.; Zhao, W.; Liu, H.-M. *J. Med. Chem.*, **2013**, *56*, 8543–8560.
50. Kutz, C. J.; Holshouser, S. L.; Marrow, E. A.; Woster, P. M. *Med. chem. Comm.*, **2014**, *5*, 1863–1870.
51. Zhou, Y.; Li, Y.; Wang, W.-J.; Xiang, P.; Luo, X.-M.; Yang, L.; Yang, S.-Y.; Zhao, Y.-L. *Bioorganic. Med. Chem. Lett.*, **2016**, *26*, 4552–4557.
52. Forneris, F.; Binda, C.; Adamo, A.; Battaglioli, E.; Mattevi, A. *J. Biol. Chem.*, **2007**, *282*, 20070–20074.
53. Yang, M.; Culhane, J. C.; Szewczuk, L. M.; Gocke, C. B.; Brautigam, C. A.; Tomchick, D. R.; Machius, M.; Cole, P. A.; Yu, H. *Nat. Struct. Mol. Biol.*, **2007**, *14*, 535–539.
54. Pfister, S. X.; Ashworth, A. *Nat. Rev. Drug Discov.*, **2017**, *16*, 241–263.
55. Bissantz, C.; Kuhn, B.; Stahl, M. *J. Med. Chem.*, **2010**, *53*, 5061–5084.
56. Kumarasinghe, I. R.; Woster, P. M. *ACS. Med. Chem. Lett.*, **2013**, *5*, 29–33.
57. Moellering, R. E.; Cornejo, M.; Davis, T. N.; Del Bianco, C.; Aster, J. C.; Blacklow, S. C.; Kung, A. L.; Gilliland, D. G.; Verdine, G. L.; Bradner, J. E. *Nature*, **2009**, *462*, 182–188.
58. Walensky, L. D.; Kung, A. L.; Escher, I.; Malia, T. J.; Barbuto, S.; Wright, R. D.; Wagner, G.; Verdine, G. L.; Korsmeyer, S. J. *Science*, **2004**, *305*, 1466–1470.
59. Walensky, L. D.; Pitter, K.; Morash, J.; Oh, K. J.; Barbuto, S.; Fisher, J.; Smith, E.; Verdine, G. L.; Korsmeyer, S. J. *Mol. Cell*, **2006**, *24*, 199–210.
60. Merrifield, R. B. *J. Am. Chem. Soc.*, **1963**, *85*, 2149–2154.
61. Dalvit, C.; Pevarello, P.; Tatò, M.; Veronesi, M.; Vulpetti, A.; Sundström, M. *J. Biomol. NMR*, **2000**, *18*, 65–68.
62. Dalvit, C.; Fogliatto, G.; Stewart, A.; Veronesi, M.; Vulpetti, A.; Stockman, B. *J. Biomol. NMR*, **2001**, *21*, 349–359.
63. Wishart, D. S.; Sykes, B. D. *J. Biomol. NMR*, **1994**, *4*, 171–180.
64. Spera, S.; Bax, A. *J. Am. Chem. Soc.*, **1991**, *113* (14), 5490–5492.
65. Wishart, D. S.; Sykes, B. D.; Richards, F. M. *J. Mol. Bio.*, **1991**, *222*, 311–333.
66. Bundi, A.; Grathwohl, C.; Hochmann, J.; Keller, R. M.; Wagner, G.; W thrich, K. *J. Magn. Reson.*, (1969) **1975**, *18*, 191–198.
67. Demchenko, A. P. *Introduction to fluorescence sensing*; Springer, Dordrecht, **2008**.
68. Enander, K.; Choulier, L.; Olsson, A. L.; Yushchenko, D. A.; Kanmert, D.; Klymchenko, A. S.; Demchenko, A. P.; Mély, Y.; Altschuh, D. *Bioconjugate Chem.*, **2008**, *19*, 1864–1870.
69. Choulier, L.; Choulier, L.; Shvadchak, V. V.; Shvadchak, V. V.; Naidoo, A.; Naidoo, A.; Klymchenko, A. S.; Mély, Y.; Altschuh, D. *Anal. Biochem.*, **2010**, *401*, 188–195.
70. Oshannessy, D. J.; Brighamburke, M.; Soneson, K. K.; Hensley, P.; Brooks, I. *Anal. Biochem.*, **1993**, *212*, 457–468.

Acta Universitatis Upsaliensis

*Digital Comprehensive Summaries of Uppsala Dissertations
from the Faculty of Science and Technology 1568*

Editor: The Dean of the Faculty of Science and Technology

A doctoral dissertation from the Faculty of Science and Technology, Uppsala University, is usually a summary of a number of papers. A few copies of the complete dissertation are kept at major Swedish research libraries, while the summary alone is distributed internationally through the series Digital Comprehensive Summaries of Uppsala Dissertations from the Faculty of Science and Technology. (Prior to January, 2005, the series was published under the title “Comprehensive Summaries of Uppsala Dissertations from the Faculty of Science and Technology”.)

Distribution: publications.uu.se
urn:nbn:se:uu:diva-330489



ACTA
UNIVERSITATIS
UPSALIENSIS
UPPSALA
2017